

A general framework for uncertainty quantification under non-Gaussian input dependencies

E. Torre^{1,2,3}, S. Marelli², P. Embrechts^{3,1,4}, and B. Sudret^{2,1}

¹*Risk Center, ETH Zurich, Switzerland*

²*Chair of Risk, Safety and Uncertainty Quantification, ETH Zurich, Stefano-Francini-Platz 5, 8093 Zurich, Switzerland*

³*RiskLab, ETH Zurich, Zurich, Switzerland*

⁴*Swiss Finance Institute, ETH Zurich, Switzerland*

Abstract

Systems subject to uncertain inputs produce uncertain responses. Uncertainty quantification (UQ) deals with the estimation of statistics of the system response, given a computational model of the system and a probabilistic model of the uncertainty in its input parameters. In engineering applications it is common to assume that the inputs are mutually independent or coupled by a Gaussian dependence structure (copula). In addition, many advanced UQ techniques rely on a transformation of the inputs into independent variables (through, *e.g.*, the Rosenblatt transform). The transform is unknown or difficult to compute in most cases, with the notable exception of the Gaussian copula, which admits a simple closed-form solution (also known as Nataf transform). This makes the Gaussian assumption widely used in UQ applications, despite being often inaccurate. In this paper we overcome such limitations by modelling the dependence structure of multivariate inputs as vine copulas. Vine copulas are models of multivariate dependence built from simpler pair-copulas. The vine representation is flexible enough to capture complex dependencies. It also allows for statistical inference of the model parameters and it provides numerical algorithms to compute the associated Rosenblatt transform. We formalise the framework needed to build vine copula models of multivariate inputs and to combine them with UQ methods. We exemplify the procedure on two realistic engineering structures, both subject to inputs with non-Gaussian dependence structures. For each case, we analyse the moments of the model response (using polynomial chaos expansions), and perform a structural reliability analysis to calculate the probability of failure of the system (using the first order reliability method). We demonstrate that the Gaussian assumption yields biased statistics, whereas the vine copula representation achieves significantly more precise estimates.

Keywords: uncertainty quantification – input dependencies – vine copulas – Rosenblatt transform

1 Introduction

Uncertainty Quantification (UQ) estimates statistics of the response of a system subject to stochastic inputs. The system is usually described by a deterministic computational model \mathcal{M} (e.g., a finite element code). The input consists of M possibly coupled parameters, modelled by a random vector \mathbf{X} with joint cumulative distribution function (CDF) $F_{\mathbf{X}}$ and probability density (PDF) $f_{\mathbf{X}}$. The computational model transforms \mathbf{X} into an uncertain output $Y = \mathcal{M}(\mathbf{X})$, which here we take to be a univariate random variable. Extensions to multivariate outputs is straightforward. Of interest in UQ problems are various statistics of Y , such as its CDF F_Y , its moments, the probability of extreme events (i.e., of small or large quantiles), the sensitivity of Y to the different components X_i of \mathbf{X} , and others. Because \mathcal{M} is typically a complex model which is not known explicitly, analytical solutions are not available. The model behavior can only be known point-wise in correspondence with inputs $\mathbf{x}^{(j)}$ sampled from $F_{\mathbf{X}}$, where it produces responses $y^{(j)} = \mathcal{M}(\mathbf{x}^{(j)})$ (non-intrusive, or black-box approach). The classical strategy to solve this class of problems is Monte Carlo simulation (MCS). MCS draws the $\mathbf{x}^{(j)}$ as i.i.d samples from $F_{\mathbf{X}}$, which requires the sample size n to be large enough to cover the input probability space sufficiently well. When \mathcal{M} is computationally expensive and the available computational budget is limited to a few dozens to hundreds of runs, alternative approximation techniques are used instead of MCS. Examples include the first and second order reliability methods (FORM, SORM), importance sampling (IS) and subset simulation in reliability analysis for the estimation of small failure probabilities Ditlevsen and Madsen (1996); Lemaire (2009), polynomial chaos expansions (PCE) and other metamodeling techniques for the estimation of moments.

Since \mathcal{M} is a deterministic code, all uncertainty in Y is due to the uncertainty in \mathbf{X} . Therefore, regardless of the approach (MCS or others) chosen to estimate the statistics of Y of interest, a suitable model of $F_{\mathbf{X}}$ is critical to obtain accurate estimates. Historically, the components X_i of \mathbf{X} are assumed to be mutually independent, or to have the dependence structure of a Gaussian multivariate distribution Lebrun and Dutfoy (2009). Gaussian distributions are simple to model and to fit to data, since they only require only the computation of pairwise correlation coefficients. In addition, some advanced UQ techniques work for mutually independent inputs only. These include FORM Hasofer and Lind (1974), SORM Fiessler et al. (1979), importance sampling Melchers (1999), some types of subset simulation (e.g. Papaioannou et al., 2015), PCE Li and Ghanem (1998), and other methods. These methods need a transformation to map the input vector \mathbf{X} onto a vector \mathbf{Z} with independent components. The most general of such transformations, the Rosenblatt transform (Rosenblatt, 1952), requires the computation of conditional PDFs, which are hardly known in practical

applications. However, when $F_{\mathbf{X}}$ has a Gaussian dependence structure, this map is known and is equivalent to the well known Nataf transform (Nataf, 1962; Lebrun and Dutfoy, 2009). The Gaussian assumption introduces thus a convenient representation of input dependencies. When the real dependence structure deviates from this assumption, it may introduce a bias in the resulting estimates. Due to the lack of alternative viable probabilistic models, however, the validity or the impact of the Gaussian assumption are typically not quantified. Novel methodologies in UQ largely focus on providing better estimation techniques rather than on allowing for different probabilistic input models.

Recently, dependence modelling has seen significant advances in the mathematical community with the widespread adoption of copula models, and of vine copulas in particular. Copula theory allows to separately model the dependence (by multivariate copula functions) and the marginal behaviour (by univariate CDFs) of joint distributions. This provides a flexible way to build multivariate probability models by choosing each ingredient individually (Nelsen, 2006; Joe, 2015). Copulas have been used in various studies, such as in earthquake (Goda, 2010; Goda and Tesfamariam, 2015; Zentner, 2017) and sea waves (Michele et al., 2007; Masina et al., 2015; Montes-Iturrizaga and Heredia-Zavoni, 2016) engineering. Applications, however, are often limited to low-dimensional problems (typically bivariate) or to relatively simple copula families, prominently the Gaussian or Archimedean families Nelsen (2006). In higher dimensions, building and selecting copulas that properly represent the coupling of the phenomena of interest may be a complex problem. Vine copulas, first established by Joe (1996) and Bedford and Cooke (2002), ease this construction by expressing multivariate copulas as a product of simpler bivariate copulas among pairs of random variables. As a result, vine models offer an easy interpretation and are extremely flexible. Vine copulas have been extensively employed, for instance, in financial applications (Aas, 2016). In engineering, these models have been, so far, largely overseen. Recently, Wang and Li (2017a,b) proposed their application in the context of reliability analysis, for the special case when only partial information (correlation coefficients) is available.

The purpose of this contribution is to show that vine copulas represent a suitable tool to model inputs in UQ problems, and to propose a general framework for their usage. Since algorithms to compute the Rosenblatt transform of vine copulas are available, these models are applicable also in combination with UQ techniques that work in probability spaces with independent variables. Algorithms to fit vine models to data, for instance based on maximum likelihood or Bayesian estimation, also exist, making these models suitable for data driven applications (Aas et al., 2009; Schepsmeier, 2015).

After recalling fundamental results of copula and vine copula theory (Sections 2-3), we re-formalise three established UQ methodologies that work for independent inputs, FORM, IS and PCE, for inputs with dependent components (Section 4). In Sections 5-6 we show on two truss models that modelling non-Gaussian input dependence with the Gaussian copula

yields wrong estimates of the failure probability and response moments. The problem cannot be amended using different UQ methods, since it is inherent to the misinterpretation of the input uncertainty. Reliable estimates are obtained instead by FORM, IS or PCE using a suitable vine representation of the input, also when the vine is purely inferred from available data.

2 Copulas and vine copulas

Multivariate inputs in UQ problems are generally modelled as random vectors. The statistical properties of an M -dimensional random vector \mathbf{X} are fully described by its joint CDF $F_{\mathbf{X}} : \mathbb{R}^M \rightarrow [0, 1]$, $\mathbf{x} \mapsto F_{\mathbf{X}}(\mathbf{x}) = \mathbb{P}(X_1 \leq x_1, \dots, X_M \leq x_M)$.

Joint CDFs define both the marginal PDFs of each component X_i of \mathbf{X} , *i.e.*, $F_i(x_i) = F_{X_i}(x_i) = \mathbb{P}(X_i \leq x_i)$, and the dependencies among the variables. As such, prescribed parametric families of joint CDFs dictate specific parametric forms for the marginal and joint properties of the random variables. More flexible models should be compatible with inference techniques, to be applicable when only a finite number of realisations of the input \mathbf{X} is available. They should also optimally provide the isoprobabilistic map that decouples their random variables, such to be usable in combination with UQ techniques that assume mutually independent inputs. This section introduces vine copula models and illustrates how they meet the requirements listed above.

2.1 Copulas and Sklar's theorem

An M -copula is defined as an M -variate joint CDF $C : [0, 1]^M \rightarrow [0, 1]$ with standard uniform marginals, that is,

$$C(1, \dots, 1, u_i, 1, \dots, 1) = u_i \quad \forall u_i \in [0, 1], \quad \forall i = 1, \dots, M.$$

Sklar's theorem (Sklar, 1959) allows one to express joint CDFs in terms of their marginal distributions and a copula.

Theorem (Sklar). *For any M -variate CDF $F_{\mathbf{X}}$ with marginals F_1, \dots, F_M , an M -copula $C_{\mathbf{X}}$ exists, such that for all $\mathbf{x} \in \mathbb{R}^M$*

$$F_{\mathbf{X}}(\mathbf{x}) = C_{\mathbf{X}}(F_1(x_1), \dots, F_M(x_M)). \quad (1)$$

Besides, $C_{\mathbf{X}}$ is unique on $\text{Ran}(F_1) \times \dots \times \text{Ran}(F_M)$, where Ran is the range operator. In particular, $C_{\mathbf{X}}$ is unique on $[0, 1]^M$ if all F_i are continuous, and it is given by

$$C_{\mathbf{X}}(\mathbf{u}) = F_{\mathbf{X}}(F_1^{-1}(u_1), \dots, F_M^{-1}(u_M)), \quad \mathbf{u} \in [0, 1]^M. \quad (2)$$

Conversely, for any M -copula C and any set of M univariate CDFs F_i with domain \mathcal{D}_i , $i = 1, \dots, M$, the function $F : \mathcal{D}_1 \times \dots \times \mathcal{D}_M \rightarrow [0, 1]$ defined by

$$F(x_1, \dots, x_M) := C(F_1(x_1), \dots, F_M(x_M)) \quad (3)$$

is an M -variate CDF with marginals F_1, \dots, F_M .

The representation (1) guarantees that any joint CDF can be expressed in terms of its marginals and a copula. In the following we work with joint CDFs $F_{\mathbf{X}}$ having continuous marginals F_i .

Copulas of known families of joint CDFs can be derived from (2). Finally, one can use (3) to build a multivariate CDF F by independently specifying and combining a copula function C and M univariate CDFs F_i . The copula describes the dependence properties, while the univariate CDFs describe the marginal behaviour. Sklar's theorem thus allows one to split the problem of modelling the joint behaviour of the components of \mathbf{X} into two separate problems, that can be treated independently. One first models the marginals F_i , then transforms the original components X_i into uniform random variables $U_i = F_i(X_i)$, leading to the transformation

$$\mathcal{T}^{(u)}(\mathbf{X}) = (F_1(X_1), \dots, F_M(X_M))^{\top}. \quad (4)$$

The joint CDF of $\mathbf{U} = (U_1, \dots, U_M)^{\top}$ is the associated copula.

Sklar's theorem can be re-stated in terms of probability densities. If \mathbf{X} admits PDF $f_{\mathbf{X}}(\mathbf{x}) := \frac{\partial^M F_{\mathbf{X}}(\mathbf{x})}{\partial x_1 \dots \partial x_M}$ and copula density $c_{\mathbf{X}}(\mathbf{x}) := \frac{\partial^M C_{\mathbf{X}}(\mathbf{u})}{\partial u_1 \dots \partial u_M}$, then the following relation holds:

$$f_{\mathbf{X}}(\mathbf{x}) = c_{\mathbf{X}}(F_1(x_1), \dots, F_M(x_M)) \cdot \prod_{i=1}^M f_i(x_i). \quad (5)$$

2.2 Copula-based measures of dependence

Since copulas fully describe multivariate dependencies, it is natural to introduce dependence measures based on the copula only, and not on the marginals. Several such measures, also known as measures of association, exist. An example is Spearman's correlation coefficient, defined for a random pair (X_1, X_2) as

$$\rho_S(X_1, X_2) := \rho_P(F_1(X_1), F_2(X_2)),$$

where ρ_P is the classical Pearson correlation coefficient. Another example is Kendall's tau

$$\tau_K(X_1, X_2) := \mathbb{P}((X_1 - \tilde{X}_1)(X_2 - \tilde{X}_2) > 0) - \mathbb{P}((X_1 - \tilde{X}_1)(X_2 - \tilde{X}_2) < 0),$$

where $(\tilde{X}_1, \tilde{X}_2)$ is an independent copy of (X_1, X_2) . If the copula of (X_1, X_2) is C , then

$$\rho_S(X_1, X_2) = 12 \int \int_{[0,1]^2} C(u, v) dudv - 3, \quad (6)$$

and

$$\tau_K(X_1, X_2) = 4 \int \int_{[0,1]^2} C(u, v) dC(u, v) - 1. \quad (7)$$

One can show that $\tau_K = 0$ and $\rho_S = 0$ if (X_1, X_2) are independent, $\tau_K = 1 \Leftrightarrow \rho_S = 1 \Leftrightarrow X_1 = \alpha(X_2)$ for some strictly increasing $\alpha(\cdot)$, and $\tau_K = -1 \Leftrightarrow \rho_S = -1 \Leftrightarrow X_2 = \beta(X_1)$ for some strictly decreasing $\beta(\cdot)$ Embrechts et al. (1999).

Other copula based measures of pairwise concordance exist (Scarsini, 1984), as well as multivariate extensions (Taylor, 2007). A discussion of such measures is beyond the scope of this paper.

Asymptotic tail dependence (hereinafter, simply tail dependence) of a random pair (X_1, X_2) is another example of dependence property that is completely described by the copula and not by the marginals. The joint distribution of (X_1, X_2) is said to be upper tail dependent if the probability that one of the two variables takes values in its upper tail (*i.e.*, high quantiles) given that other has taken values in its upper range does not decay to zero. Lower tail dependence is defined analogously for low quantiles. Tail dependence thus allows for simultaneous extremes, and is for instance used to model systemic risks. Formally, (X_1, X_2) with marginals F_1 and F_2 are upper tail dependent if

$$\lim_{u \uparrow 1^-} \mathbb{P}(X_1 > F_1^{-1}(u) | X_2 > F_2^{-1}(u)) = \lambda_u > 0, \quad (8)$$

and are lower tail dependent if

$$\lim_{u \downarrow 0^+} \mathbb{P}(X_1 < F_1^{-1}(u) | X_2 < F_2^{-1}(u)) = \lambda_l > 0, \quad (9)$$

given that these limits exist; λ_u and λ_l are called the upper and lower tail dependence coefficients, and are given by

$$\lambda_u = \lim_{u \uparrow 1^-} \frac{1 - 2u + C(u, u)}{1 - u}, \quad \lambda_l = \lim_{u \downarrow 0^+} \frac{C(u, u)}{u}. \quad (10)$$

2.3 Copula examples

Here we provide three families of copulas that will be used in Section 5 and Section 6 to model different dependence structures among input loads on a truss model. A list of classical families of bivariate pair copulas and their properties can be found in (Nelsen, 2006; Joe, 2015).

The independence copula

$$C^{(\Pi)} : [0, 1]^M \rightarrow [0, 1], \quad (u_1, \dots, u_M) \mapsto \prod_{i=1}^M u_i \quad (11)$$

describes the case of mutual independence among M random variables. For $M = 2$, $C^{(\Pi)}$ has Spearman's rho $\rho_S^{(\Pi)} = 0$, Kendall's tau $\tau_K^{(\Pi)} = 0$, and the tail dependence coefficients $\lambda_u^{(\Pi)} = \lambda_l^{(\Pi)} = 0$.

A Gaussian random vector \mathbf{X} with correlation matrix $\mathbf{R} = (\rho_{ij})_{i,j=1}^M$ and marginals $F_i \sim \mathcal{N}(\mu_i, \sigma_i^2)$, $i = 1, \dots, M$, has copula

$$C^{(\mathcal{N})}(\mathbf{u}) = \frac{1}{\sqrt{\det \mathbf{R}}} \exp \left(-\frac{1}{2} \begin{pmatrix} \Phi^{-1}(u_1) \\ \vdots \\ \Phi^{-1}(u_M) \end{pmatrix}^T \cdot (\mathbf{R}^{-1} - \mathbf{I}) \cdot \begin{pmatrix} \Phi^{-1}(u_1) \\ \vdots \\ \Phi^{-1}(u_M) \end{pmatrix} \right), \quad (12)$$

where Φ is the standard normal CDF and \mathbf{I} is the identity matrix. $C^{(\mathcal{N})}$ is called Gaussian copula or normal copula. One can prove that, if $M \geq 3$ variables are coupled by a Gaussian copula with correlation matrix \mathbf{R} , any pairs (X_i, X_j) are coupled by a Gaussian pair copula with correlation matrix $\begin{bmatrix} 1 & \rho_{ij} \\ \rho_{ij} & 1 \end{bmatrix}$. If so, their Spearman's rho is $\rho_S^{(\mathcal{N})} = \frac{6}{\pi} \arcsin(\frac{\rho_{ij}}{2})$, their Kendall's tau is $\tau_K^{(\mathcal{N})} = \frac{2}{\pi} \arcsin(\rho_{ij})$, and their tail dependence coefficients are $\lambda_u^{(\mathcal{N})} = \lambda_l^{(\mathcal{N})} = 0$. Therefore, multivariate Gaussian copulas assign negligible probabilities to joint extremes.

A pair copula that contemplates upper tail dependence is the bivariate Gumbel-Hougaard copula

$$C^{(\mathcal{GH})}(u, v) = \exp\left(-[(-\log u)^\theta + (-\log v)^\theta]^{1/\theta}\right), \quad \theta \in [1, +\infty). \quad (13)$$

In particular, if $\theta = 1$ then $C^{(\mathcal{GH})}(u, v) = uv$ (the independence copula). $C^{(\mathcal{GH})}$ has Kendall's tau $\tau_K^{(\mathcal{GH})} = (\theta - 1)/\theta$ and upper tail dependence coefficient $\lambda_u^{(\mathcal{GH})} = 2 - 2^{1/\theta}$, which increases from 0 to 1 as θ increases from 1 to $+\infty$. Finally, $\lambda_l^{(\mathcal{GH})} = 0$.

2.4 Vine copulas

When the input dimension M grows, defining a suitable M -copula which properly describes the pairwise and higher-order dependencies among the input variables becomes increasingly difficult. Multivariate extensions of several families of pair-copulas exist, but they rarely fit real data well. Bedford and Cooke (2002) proved that, instead, one may construct any M -copula by a product of simpler 2-copulas. Some are unconditional copulas among pairs of random variables, others are conditioned on the values taken by other variables. Here we briefly introduce this construction, known as pair copula construction or vine construction, and recall some important features. For details, we refer to the cited literature (see also Klüpperberg and Czado (date)). A recent review with a focus on financial applications can be found in Aas (2016).

Let $\mathbf{u}_{\bar{i}}$ be the vector obtained from the vector \mathbf{u} by removing its i -th component, *i.e.*, $\mathbf{u}_{\bar{i}} = (u_1, \dots, u_{i-1}, u_{i+1}, \dots, u_M)^T$. Similarly, let $\mathbf{u}_{\overline{\{i,j\}}}$ be the vector obtained by removing the i -th and j -th component, and so on. For a general subset $\mathcal{A} \subset \{1, \dots, M\}$, $\mathbf{u}_{\overline{\mathcal{A}}}$ is defined analogously. Also, $F_{\overline{\mathcal{A}}|\mathcal{A}}$ and $f_{\overline{\mathcal{A}}|\mathcal{A}}$ indicate the joint CDF and PDF of the random vector $\mathbf{X}_{\overline{\mathcal{A}}}$ conditioned on $\mathbf{X}_{\mathcal{A}}$; $\mathcal{A} = \{i_1, \dots, i_k\}$ and $\overline{\mathcal{A}} = \{j_1, \dots, j_l\}$ form a partition of $\{1, \dots, M\}$, that is, $\mathcal{A} \cup \overline{\mathcal{A}} = \{1, \dots, M\}$ and $\mathcal{A} \cap \overline{\mathcal{A}} = \emptyset$.

Using (5), $f_{\overline{\mathcal{A}}|\mathcal{A}}$ can be expressed as

$$\begin{aligned} f_{\overline{\mathcal{A}}|\mathcal{A}}(\mathbf{x}_{\overline{\mathcal{A}}}|\mathbf{x}_{\mathcal{A}}) &= c_{\overline{\mathcal{A}}|\mathcal{A}}(F_{j_1|\mathcal{A}}(x_{j_1}|\mathbf{x}_{\mathcal{A}}), F_{j_2|\mathcal{A}}(x_{j_2}|\mathbf{x}_{\mathcal{A}}), \dots, F_{j_l|\mathcal{A}}(x_{j_l}|\mathbf{x}_{\mathcal{A}})) \times \\ &\quad \times \prod_{j \in \overline{\mathcal{A}}} f_{j|\mathcal{A}}(x_j|\mathbf{x}_{\mathcal{A}}), \end{aligned} \quad (14)$$

where $c_{\overline{\mathcal{A}}|\mathcal{A}}$ is an l -copula density – that of the conditional random variables $(X_{j_1|\mathcal{A}}, X_{j_2|\mathcal{A}}, \dots, X_{j_l|\mathcal{A}})^T$ – and $f_{j|\mathcal{A}}$ is the conditional PDF of X_j given $\mathbf{X}_{\mathcal{A}}$, $j \in \overline{\mathcal{A}}$. Following Joe (1996), the

univariate conditional distributions $F_{j|\mathcal{A}}$ can be further expressed in terms of any conditional pair copula $C_{ji|\mathcal{A}\setminus\{i\}}$ between $X_{j|\mathcal{A}\setminus\{i\}}$ and $X_{i|\mathcal{A}\setminus\{i\}}$, $i \in \mathcal{A}$:

$$F_{j|\mathcal{A}}(x_j|\mathbf{x}_{\mathcal{A}}) = \frac{\partial C_{ji|\mathcal{A}\setminus\{i\}}(u_j, u_i)}{\partial u_i} \Big|_{(F_{j|\mathcal{A}\setminus\{i\}}(x_j|\mathbf{x}_{\mathcal{A}\setminus\{i\}}), F_{i|\mathcal{A}\setminus\{i\}}(x_i|\mathbf{x}_{\mathcal{A}\setminus\{i\}}))}. \quad (15)$$

An analogous relation readily follows for conditional densities:

$$\begin{aligned} f_{j|\mathcal{A}}(x_j|\mathbf{x}_{\mathcal{A}}) &= \frac{\partial F_{j|\mathcal{A}}(x_j|\mathbf{x}_{\mathcal{A}})}{\partial x_j} \\ &= c_{ji|\mathcal{A}\setminus\{i\}}(F_{j|\mathcal{A}\setminus\{i\}}(x_j|\mathbf{x}_{\mathcal{A}\setminus\{i\}}), F_{i|\mathcal{A}\setminus\{i\}}(x_i|\mathbf{x}_{\mathcal{A}\setminus\{i\}})) \times \\ &\quad \times f_{j|\mathcal{A}\setminus\{i\}}(x_j|\mathbf{x}_{\mathcal{A}\setminus\{i\}}). \end{aligned} \quad (16)$$

Substituting iteratively (15)-(16) into (14), Bedford and Cooke (2002) expressed $f_{\mathbf{X}}$ as a product of pair copula densities multiplied by $\prod_i f_i$. Recalling (5), it readily follows that the associated joint copula density c can be factorised into pair copula densities. Copulas expressed in this format are called vine copulas.

The factorisation is not unique: the pair copulas involved in the construction depend on the variables chosen in the conditioning equations (15)-(16) at each iteration. To organise them, Bedford and Cooke (2002) introduced a graphical model called the regular vine (R-vine). An R-vine among M random variables is represented by a graph consisting of $M - 1$ trees T_1, T_2, \dots, T_{M-1} , where each tree T_i consists of a set N_i of nodes and a set E_i of edges $e = (j, k)$ between nodes j and k . The trees T_i satisfy the following three conditions:

1. Tree T_1 has nodes $N_1 = \{1, \dots, M\}$ and $M - 1$ edges E_1
2. for $i = 2, \dots, M - 1$, the nodes of T_i are the edges of T_{i-1} : $N_i = E_{i-1}$
3. Two edges in tree T_i can be joined as nodes of tree T_{i+1} by an edge only if they share a common node in T_i (proximity condition)

To built an R-vine with nodes $\mathcal{N} = \{N_1, \dots, N_{M-1}\}$ and edges $\mathcal{E} = \{E_1, \dots, E_{M-1}\}$, one defines for each edge e linking nodes $j = j(e)$ and $k = k(e)$ in tree T_i , the sets $I(e)$ and $D(e)$ as follows:

- If $e \in E_1$ (edge of tree T_1), then $I(e) = \{j, k\}$ and $D(e) = \emptyset$,
- If $e \in E_i$, $i \geq 2$, then $D(e) = D(j) \cup D(k) \cup (I(j) \cap I(k))$ and $I(e) = (I(j) \cup I(k)) \setminus D(e)$.

$I(e)$ contains always two indices j_e and k_e , while $D(e)$ contains $i - 1$ indices for $e \in E_i$. One then associates each edge e with the conditional pair copula $C_{j_e, k_e|D(e)}$ between X_{j_e} and X_{k_e} conditioned on the variables with indices in $D(e)$. An R-vine with M nodes can thus be expressed as Aas (2016)

$$c(\mathbf{u}) = \prod_{i=1}^{M-1} \prod_{e \in E_i} c_{j_e, k_e|D(e)}(u_{j_e|D(e)}, u_{k_e|D(e)}). \quad (17)$$

Two special classes of R-vines are the drawable vine (D-vine; Kurowicka and Cooke, 2005) and the canonical vine (C-vine; Aas et al., 2009). Denoting $F(x_i) = u_i$ and $F_{i|\mathcal{A}}(x_i|\mathbf{x}_{\mathcal{A}}) =$

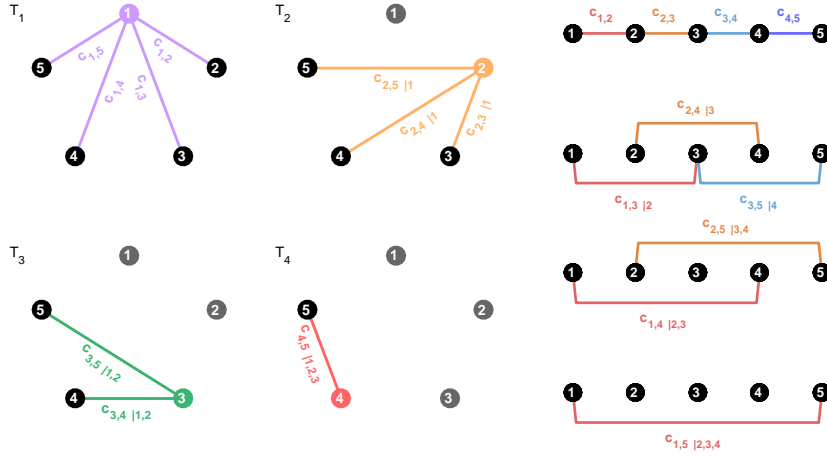


Figure 1: **Graphical representation of C- and D-vines.** The pair copulas in each tree of a 5-dimensional C-vine (left; conditioning variables are shown in grey) and of a 5-dimensional D-vine (right; conditioning variables are those between the connected nodes).

$u_{i|\mathcal{A}}$, $i \notin \mathcal{A}$, a C-vine is given by the expression

$$c(\mathbf{u}) = \prod_{j=1}^{M-1} \prod_{i=1}^{M-j} c_{j,j+i|\{1,\dots,j-1\}}(u_{j|\{1,\dots,j-1\}}, u_{j+i|\{1,\dots,j-1\}}), \quad (18)$$

while a D-vine is expressed as

$$c(\mathbf{u}) = \prod_{j=1}^{M-1} \prod_{i=1}^{M-j} c_{i,i+j|\{i+1,\dots,i+j-1\}}(u_{i|\{i+1,\dots,i+j-1\}}, u_{i+j|\{i+1,\dots,i+j-1\}}). \quad (19)$$

The graphs associated to a 5-dimensional C-vine and to a 5-dimensional D-vine are shown in Figure 1. Note that this simplified illustration differs from the standard one introduced by Aas et al. (2009) and commonly used in the literature.

2.5 Vine construction and inference in practice

Building a vine copula model involves the following steps:

1. Selecting a vine structure (for C- and D-vines: selecting the order of the nodes)
2. Selecting the pair-copula families
3. Assigning the copula parameters (from prior knowledge, or by fitting to available data)

Steps 1-2 solve the representation problem. Step 3 typically involves inference on a sample $\{\hat{\mathbf{x}}^{(1)}, \dots, \hat{\mathbf{x}}^{(n)}\}$ of observations of the input. Aas et al. (2009) provided algorithms to compute the likelihood of a C- or D-vine model given data. Joe (2015) presented a likelihood estimation algorithm for general R-vines. These algorithms enable inference based

on maximum likelihood. Bayesian methods for vine copula inference also exist Min and Czado (2011); Gruber and Czado (2015).

To facilitate inference a *simplifying assumption* is usually made, namely that the pair copulas $C_{j(e),k(e)|D(e)}$ in (17) only depend on the variables with indices in $D(e)$ through the arguments $F_{i(e)|D(e)}$ and $F_{j(e)|D(e)}$. While being exact only in particular cases, this assumption is usually not severe (Haff et al., 2010). Stöber et al. (2013) proposed construction techniques for non-simplified vine copulas.

Inference and representation may come in a loop. One may compute the likelihood of different vine representations (each defined by a class, a structure and a set of comprising pair copulas) and select the one with maximum likelihood. An alternative to likelihood maximisation is the minimisation of the Akaike information criterion (AIC)

$$\text{AIC} = -2 \log L + 2k,$$

where k is the total number of parameters of the vine copula and $\log L$ is its log-likelihood. The AIC penalises models with a larger number of parameters (which typically yield higher likelihood and would otherwise be preferred). Alternatives to the AIC have been proposed, for instance the Bayesian information criterion (BIC) and the copula information criterion (CIC; Grønneberg and Hjort, 2014). Also, one may opt for various goodness of fit tests (Schepsmeier, 2015; Fermanian, 2012). Manner (2007) showed that, among four different copula selection criteria considered, AIC is preferable.

The examples shown in the current study are restricted to C-vines (18) and D-vines (19), which cover already a large number of different dependence structures. The workflow proposed in Section 4, however, applies to any R-vine. In dimension $M = 3$, a C-vine is also a D-vine and vice versa. When $M > 3$, C-vines and D-vines always differ. The vine class may be chosen depending on known relations among the variables. For instance, if one variable represents the driving cause of existing dependencies, a C-vine whose first node is that variable may be a convenient representation. If all variables are to be treated equally in absence of further knowledge, a D-vine may provide the best representation. The vine structure may be selected after analogous considerations. Appropriate families of pair copulas could be selected based on expert knowledge.

Different vine structures, while theoretically equivalent, may provide different end results when inference takes place. On the other hand, iterating the fitting procedure over all possible structures is typically computationally prohibitive: an M -copula density admits $2^{\binom{M-2}{2}-1} M!$ different R-vine factorisations (Morales-Nápoles, 2011), $M!$ of which are C- or D- vines. Heuristic approaches have been suggested to pre-determine the optimal structure before proceeding to steps 3-4. The approach we follow in this study, originally proposed by Aas et al. (2009), consists in ordering the variables X_i such that pairs (X_i, X_j) with the strongest dependence are captured first, *i.e.*, fall in the first trees of the vine. We take the Kendall's tau $\tau_{K;i,j}$ given by (7) as the measure of dependence. For a C-vine, this means

selecting the central node in tree T_1 as the variable X_{i_1} that maximises $\sum_{j \neq i_1} \tau_{K;i_1j}$, then the node of tree T_2 as the variable X_{i_2} which maximises $\sum_{j \notin \{i_1, i_2\}} \tau_{K;i_2j}$, and so on. For a D-vine, this means ordering the variables $X_{i_1}, X_{i_2}, \dots, X_{i_M}$ in the first tree so as to maximise $\sum_{k=1}^{M-1} \tau_{K;i_k i_{k+1}}$, which we solve as an open travelling salesman problem (OTSP) (Applegate et al., 2006). An open source Matlab implementation of a genetic algorithm to solve the OTSP is provided by Kirk (2014). An algorithm to find the optimal structure for R-vines has been proposed by Dißmann et al. (2013).

Once the optimal structure has been pre-determined with the heuristics above, the AIC criterion can be used to select the best pair copulas composing the vine from a set of proposed families. This step may also be computationally prohibitive if the set of proposed families or the dimension M of the input are large. Following Aas et al. (2009), one typically first selects each pair copula separately, by finding the maximum likelihood estimates of each proposed family and by selecting the minimum-AIC pair-copula (sequential fitting). Afterwards, one keeps the selected pair-copula families and performs a global fitting of its parameters.

3 Vine representations for UQ methods assuming independent inputs

Some advanced UQ techniques work for inputs \mathbf{X} with independent components. For instance, PCE (Section 4.2) exploits this property to build polynomial basis functions which are orthogonal with respect to $F_{\mathbf{X}}$. FORM and SORM (Section 4.3), as well as other reliability methods, take advantage of the probability measure of the standard normal space to approximate low probability mass regions. When the components of \mathbf{X} are mutually dependent, these methods need a transformation \mathcal{T} that maps \mathbf{X} into \mathbf{Z} with independent components. \mathcal{T} therefore changes the copula $C_{\mathbf{X}}$ of \mathbf{X} into the independence copula $C^{(\Pi)}$ defined in (11). When \mathcal{T} also makes $F_{\mathbf{Z}}$ rotationally invariant, it is called an isoprobabilistic transform. This section discusses existing isoprobabilistic transformations, relates them to copula theory, and highlights the existence of algorithms for their computation when $C_{\mathbf{X}}$ is an R-vine. By doing so, we demonstrate that vine copulas provide effective models of complex input dependencies also in combination with UQ methods that rely on an isoprobabilistic transform of the input.

3.1 Compositional models for dependent inputs

Consider a generic UQ method that works in a probability space where input parameters are independent and have marginal distributions G_i . Assume that the input \mathbf{X} to the model \mathcal{M} has a joint CDF $F_{\mathbf{X}}$ for which an invertible isoprobabilistic transform $\mathcal{T} : \mathbf{X} \mapsto \mathbf{Z}$ is known, and that $\mathcal{T}^{-1} : \mathbf{Z} \mapsto \mathbf{X}$ is also known. Then, the system response $Y = \mathcal{M}(\mathbf{X})$ can be expressed as a function of \mathbf{Z} by

$$Y = (\mathcal{M} \circ \mathcal{T}^{-1})(\mathbf{Z}). \quad (20)$$

The *compositional model* $\mathcal{M} \circ \mathcal{T}^{-1}$ can be seen as a black box model which combines the known map \mathcal{T}^{-1} with the original computational model \mathcal{M} . The UQ method of choice can then be applied on the input \mathbf{Z} and the model $\mathcal{M} \circ \mathcal{T}^{-1}$: the statistics of the output of $\mathcal{M} \circ \mathcal{T}^{-1}$ in response to \mathbf{Z} are identical to the statistics of the output of \mathcal{M} in response to \mathbf{X} .

Given $F_{\mathbf{X}}$ and \mathcal{M} , determining the compositional model requires then to determine \mathcal{T}^{-1} , which depends on $F_{\mathbf{X}}$. However, a general closed form expression for \mathcal{T}^{-1} is in most cases unknown, even when $F_{\mathbf{X}}$ is known. This problem is associated exclusively to the copula $C_{\mathbf{X}}$ of \mathbf{X} , and not to its marginals F_i . Indeed, \mathbf{X} can be mapped by the transformation $\mathcal{T}^{(\mathcal{U})}$ defined in (4) onto $\mathbf{U} \sim U([0, 1]^M)$, whose joint CDF is $C_{\mathbf{X}}$. Thus, one can always write

$$\mathcal{T} = \mathcal{T}^{(\mathcal{U})} \circ \mathcal{T}^{(\Pi)}, \quad (21)$$

where $\mathcal{T}^{(\mathcal{U})}$ – which depends on the marginals only – is known for a given $F_{\mathbf{X}}$, while $\mathcal{T}^{(\Pi)} : \mathbf{U} \mapsto \mathbf{Z}$ is to be determined.

3.2 Isoprobabilistic transforms and copulas

The most general isoprobabilistic transform \mathcal{T} , valid for any continuous $F_{\mathbf{X}}$, is the Rosenblatt transform (Rosenblatt, 1952), which reads

$$\mathcal{T}_1^{(\mathcal{R})} : \mathcal{D}_{\mathbf{X}} \rightarrow [0, 1]^M, \mathbf{X} \mapsto \mathbf{W}, \text{ where } \begin{cases} W_1 = F_1(X_1) \\ W_2 = F_{2|1}(X_2|X_1) \\ \vdots \\ W_M = F_{M|1,\dots,M-1}(X_M|X_1, \dots, X_{M-1}) \end{cases} \quad (22)$$

Following (21), one can rewrite $\mathcal{T}_1^{(\mathcal{R})} = \mathcal{T}_1^{(\Pi, \mathcal{R})} \circ \mathcal{T}^{(\mathcal{U})}$, where

$$\mathcal{T}_1^{(\Pi, \mathcal{R})} : [0, 1]^M \rightarrow [0, 1]^M, \mathbf{U} \mapsto \mathbf{W}, \text{ with } W_i = C_{i|1,\dots,i-1}(U_i|U_1, \dots, U_{i-1}). \quad (23)$$

Here, $C_{i|1,\dots,i-1}$ are conditional copulas of \mathbf{X} (and therefore of \mathbf{U}), obtained from $C_{\mathbf{X}}$ by differentiation. The problem of obtaining an isoprobabilistic transform of \mathbf{X} is thus reduced to the problem of computing derivatives of $C_{\mathbf{X}}$.

The variables W_i are mutually independent and marginally uniformly distributed in $[0, 1]$. To assign W_i any other marginal distribution Ψ_i , one can define the generalised Rosenblatt transform as a map $\mathcal{T}^{(\mathcal{R})} = \mathcal{T}_2^{(\mathcal{R})} \circ \mathcal{T}_1^{(\mathcal{R})} = \mathcal{T}_2^{(\mathcal{R})} \circ \mathcal{T}_1^{(\Pi, \mathcal{R})} \circ \mathcal{T}^{(\mathcal{U})}$, where

$$\mathcal{T}_2^{(\mathcal{R})}(\mathbf{W}) = \mathbf{Z}, \text{ with } Z_i = \Psi_i^{-1}(W_i). \quad (24)$$

When $\Psi_i = F_i$ for all i , *i.e.*, $\mathcal{T}_2^{(\mathcal{R})} = (\mathcal{T}^{(\mathcal{U})})^{-1}$, $\mathcal{T}^{(\mathcal{R})}$ maps \mathbf{X} onto a random vector \mathbf{Z} with same marginals but independent components.

Each continuous joint CDF $F_{\mathbf{X}}$ defines multiple transforms of the type (23), one per permutation of the indices $\{1, \dots, M\}$. However, these transforms involve conditional probabilities which are not generally available in closed form. A notable exception is the Gaussian joint CDF, where independence can be obtained by diagonalisation of the correlation matrix (*e.g.*, by Choleski decomposition). The Rosenblatt transform in this case (and in this case only) is equivalent to the Nataf transform (Nataf, 1962), which is commonly used in engineering applications. Adopting the Nataf transform instead of the Rosenblatt transform for inputs with non-Gaussian copulas may cause non negligible errors.

3.3 Rosenblatt transform of R-vines

Aas et al. (2009) provided algorithms to compute the Rosenblatt transform (23) and its inverse when $C_{\mathbf{X}}$ is a given C- or D-vine. Given the pair-copulas C_{ij} in the first tree of the vine, the algorithms first compute their derivatives $C_{i|j}$. Higher-order derivatives $C_{i|ijk}$, $C_{i|ijkh}, \dots$ are obtained from the lower-order ones and their inverses by iteration. Derivatives and inverses of continuous pair copulas are available analytically in few cases (such as the Gaussian and the t-copula) and computationally cheap to compute numerically otherwise. The algorithms, provided in the original reference for a single sample point, can be trivially implemented such that n samples are processed in parallel. The functions involved are pair copula distributions, their inverses and their derivatives. An algorithm for the computation of the Rosenblatt and inverse Rosenblatt transforms for general R-vines was proposed by Schepsmeier (2015).

In addition, $(\mathcal{T}^{(\mathcal{R})})^{-1}$ allows to sample from the vine model by transforming independent points uniformly distributed in $[0, 1]^M$. Space filling samples can be obtained analogously (*e.g.*, by Sobol quasi-random sequences or Latin Hypercube sampling, McKay et al. (1979)). Given in particular a vine model of the input dependencies (obtained, *e.g.*, from expert knowledge or by inference from available data), the inverse Rosenblatt transform enables resampling.

4 UQ for inputs with a non-Gaussian copula

After recalling convergence properties of MC estimates, we summarise here three established UQ methods, polynomial chaos expansion (PCE), the first order reliability method (FORM), and importance sampling (IS), which work for independent inputs. PCE is a spectral method that expresses the system response as a polynomial of the input. It is used to estimate moments of the response, to compute sensitivity indices, or to perform resampling efficiently. FORM is a reliability analysis method designed to approximate small failure probabilities P_f numerically. IS is a stochastic sampling method that combines FORM with MC to obtain more robust estimates of P_f . When the computational budget is limited and only few

$\eta(\cdot)$:	$\mu(Y) = \int_{\mathbb{R}} y f_Y(y) dy$	$\sigma(Y) = \sqrt{\int_{\mathbb{R}} (y - \mu(Y))^2 f_Y(y) dy}$	$P_{f;y^*}(Y) = \int_{\{Y \geq y^*\}} f_Y(y) dy$
$\hat{\eta}_n(\cdot)$:	$\hat{\mu}_n(Y) = \frac{1}{n} \sum_j \hat{y}^{(j)}$	$\hat{\sigma}_n(Y) = \sqrt{\frac{1}{n-1} \sum_j (\hat{y}^{(j)} - \hat{\mu}_n(Y))^2}$	$\hat{P}_{f;y^*}(Y) = \frac{1}{n} \sum_j \mathbf{1}_{\{\hat{y}^{(j)} > y^*\}}$
CoV($\hat{\eta}_n$):	$\frac{\sigma(Y)}{\mu(Y)} \frac{1}{\sqrt{n}}$	$\approx \frac{1}{\sqrt{2n}}$	$\sqrt{\frac{1 - P_f}{nP_f}}$

Table 1: **Some MC sample estimates and their CoV.** The first row of the table defines the mean, standard deviation, and failure probability of the random variable Y . The second row shows their sample estimators, and the bottom row the CoV of such estimators (exact for $\hat{\sigma}_n(Y)$ only if Y is normally distributed).

runs of the computational model can be afforded, these methods provide significantly better estimates of their target statistics than MCS on the same number of observations. However, a strong pre-requisite is that the input random vector is, or can be mapped onto, a vector with independent components.

Here we combine both PCE and FORM with the vine representation of the input CDF illustrated in Section 2. The flexibility of R-vine models expands the applicability of these methods drastically.

4.1 Convergence of MC estimates

MC (or sample) estimates of a statistic $\eta = \eta(Y)$ are obtained as functions $\hat{\eta}_n = \hat{\eta}_n(Y)$ of n i.i.d realizations $\{\hat{y}^{(j)}\}_{j=1}^n$ of Y . Three statistics considered in the applications in Sections 5-6 are the mean $\mu(Y)$ of Y , its standard deviation $\sigma(Y)$, and failure probabilities of the type $P_{f;y^*}(Y) = \mathbb{P}(Y \geq y^*)$, where y^* is a critical threshold. Their sample estimators are the sample mean $\hat{\mu}_n(Y)$, the corrected sample standard deviation $\hat{\sigma}_n(Y)$, and the sample survival function evaluated at y^* , $\hat{P}_{f;y^*,n}(Y)$. Their analytical expression is given in Table 1, first row.

If $\hat{\eta}_n(Y)$ is an unbiased estimator of $\eta(Y)$ and $\eta(Y) \neq 0$, the reliability of $\hat{\eta}_n(Y)$ can be quantified by its coefficient of variation (CoV), given by

$$\text{CoV}(\hat{\eta}_n(Y)) = \frac{\sigma(\hat{\eta}_n(Y))}{\mu(\hat{\eta}_n(Y))} = \frac{\sigma(\hat{\eta}_n(Y))}{\eta(Y)}.$$

It is common in engineering applications to accept estimates whose CoV is not larger than 0.1 (10%). The CoV of all statistics in Table 1 (second row; approximate for $\hat{\sigma}_n(Y)$) is proportional to $1/\sqrt{n}$ and thus decays to 0 when n grows, however at a slow pace. (The expression for $\text{CoV}(\hat{\sigma}_n(Y))$ is obtained from the fact that $\sigma(\hat{\sigma}_Y) = \sigma(Y)/\sqrt{2N + O(N^2)}$ if Y is normally distributed; see Romanovsky (1925)).

4.2 Polynomial Chaos Expansion

Polynomial chaos expansion (PCE) is a spectral method that represents a model \mathcal{M} of finite variance as a linear sum of orthogonal polynomials (Ghanem and Spanos, 2003; Xiu and Karniadakis, 2002). As such, the parameters of the resulting representation have a statistical interpretation. For instance, the first two moments of the PCE model are encoded in the coefficients of the obtained polynomial. The model is also computationally cheap to evaluate, enabling an efficient evaluation of other global statistics of Y (higher order moments, the PDF, *etc.*) that would otherwise require a huge number of runs of \mathcal{M} .

PCE requires independent inputs. If \mathbf{X} has non mutually independent components, it first needs to be mapped onto such a vector \mathbf{Z} by an isoprobabilistic transform. Modelling its copula $C_{\mathbf{X}}$ as an R-vine provides the Rosenblatt transform (23)-(24) needed to this end.

Given an isoprobabilistic transform \mathcal{T} such that $\mathbf{Z} = \mathcal{T}(\mathbf{X})$, it follows that $Y = (\mathcal{M} \circ \mathcal{T}^{-1})(\mathbf{Z}) = \mathcal{M}'(\mathbf{Z})$. In the following, Y is assumed to have finite variance. The polynomial chaos expansion of $Y = \mathcal{M}'(\mathbf{Z})$ is defined as

$$Y = \sum_{\alpha \in \mathbb{N}^M} y_{\alpha} \Psi_{\alpha}(\mathbf{Z}), \quad (25)$$

where the Ψ_{α} are multivariate polynomials orthonormal with respect to $f_{\mathbf{Z}}$, *i.e.*,

$$\int_{\mathcal{D}_{\mathbf{Z}}} \Psi_{\alpha}(\mathbf{z}) \Psi_{\beta}(\mathbf{z}) f_{\mathbf{Z}}(\mathbf{z}) d\mathbf{z} = \delta_{\alpha\beta}.$$

Here, $\delta_{\alpha\beta}$ is the Kroenecker delta symbol.

Since \mathbf{Z} has independent components, each Ψ_{α} can be obtained as a tensor product of M univariate polynomials $\phi_{\alpha_i}^{(i)}(x_i)$ orthonormal with respect to the marginals g_i of Z_i :

$$\Psi_{\alpha}(\mathbf{z}) = \prod_{i=1}^M \phi_{\alpha_i}^{(i)}(z_i).$$

For instance, the $\phi_{\alpha_i}^{(i)}$ are Hermite polynomials if Z_i is standard normal, *i.e.*, if $g_i(z) = \varphi(z) = \exp(-z^2/2)/\sqrt{2\pi}$. In the applications illustrated in Section 5 we work with this choice, although other choices may be favoured in other applications. An investigation of optimal choices for the marginal distributions of \mathbf{Z} is an open question that will be investigated in a future study. Classical families of polynomials are described in Xiu and Karniadakis (2002).

The sum in (25) comprises an infinite number of terms. For practical purposes, it is truncated to a finite sum (Marelli and Sudret, 2017). Given a truncation scheme and the corresponding set \mathcal{A} of multi-indices, the coefficients y_{α} in

$$Y_{PC}(\mathbf{Z}) = \sum_{\alpha \in \mathcal{A}} y_{\alpha} \Psi_{\alpha}(\mathbf{Z}) \quad (26)$$

are evaluated on a set $\{(\hat{\mathbf{z}}^{(j)} = \mathcal{T}^{-1}(\hat{\mathbf{x}}^{(j)}), \hat{y}^{(j)})\}_{j=1}^n$ of observations (the *experimental design*). Many strategies exist to accomplish this task, such as projection methods based on Gaussian

(Le Maître et al., 2001) or sparse Keese and Matthies (2003); Xiu (2010) quadrature, least-squares minimisation (Berveiller et al., 2006), and different adaptive sparse methods Doostan and Owhadi (2011); Jakeman et al. (2015), hybridised into a single methodology by Blatman and Sudret (2011). The latter is particularly suitable when M is large, because it achieves a sparse basis out of a very large initial set of possible polynomials, and is therefore the method of choice in this study.

Once a PCE metamodel (26) of the compositional model \mathcal{M}' is built, the first two moments of the response are encoded in the coefficients of the expansions. Indeed, due to orthonormality of the polynomial basis,

$$\mu(Y_{PC}) = y_0, \quad \sigma^2(Y_{PC}) = \sum_{\alpha \in \mathcal{A} \setminus \{\mathbf{0}\}} y_\alpha^2. \quad (27)$$

Higher-order moments, as well as other statistics, can be efficiently estimated by simulation.

4.3 FORM

Let $Y = \mathcal{M}(\mathbf{X})$ be the uncertain, scalar output of the computational model \mathcal{M} in response to an uncertain M -variate input \mathbf{X} with joint CDF $F_{\mathbf{X}}$, joint PDF $f_{\mathbf{X}}$ and domain $\mathcal{D}_{\mathbf{X}}$. Suppose that the system fails if $Y \geq y^*$, where y^* is a critical threshold. The failure condition is usually rewritten as $g(\mathbf{x}) \leq 0$, with $g(\mathbf{x}) = y^* - \mathcal{M}(\mathbf{x})$.

Reliability analysis concerns the evaluation of the failure probability $P_f = \mathbb{P}(g(\mathbf{X}) \leq 0)$, *i.e.*, of the probability mass over the failure domain $\mathcal{D}_f = \{\omega : g(\mathbf{X}(\omega)) \leq 0\}$. \mathcal{D}_f is typically known only implicitly, preventing a direct estimation of P_f .

Using the indicator function

$$\mathbf{1}_{\mathcal{D}_f}(\mathbf{x}) = \begin{cases} 1 & \text{if } g(\mathbf{x}) \leq 0 \\ 0 & \text{if } g(\mathbf{x}) > 0 \end{cases},$$

P_f can be expressed as

$$P_f = \int_{\mathcal{D}_{\mathbf{X}}} \mathbf{1}_{\mathcal{D}_f}(\mathbf{x}) f_{\mathbf{X}}(\mathbf{x}) d\mathbf{x} = \mu(\mathbf{1}_{\mathcal{D}_f}(\mathbf{X})), \quad (28)$$

where $\mu(\cdot)$ is the mean operator with respect to $f_{\mathbf{X}}$.

If \mathbf{X} is multivariate standard normal, FORM (Hasofer and Lind, 1974; Hohenbichler and Rackwitz, 1983) approximates \mathcal{D}_f with an hyperplane tangent to the limit-state surface $\{\omega : g(\mathbf{X}(\omega)) = 0\}$ in its point closest to the origin (the *design point* \mathbf{x}^*). Otherwise, \mathbf{X} is first mapped by an isoprobabilistic transformation \mathcal{T} (Section 3.2) into a standard normal random vector $\mathbf{Z} = \mathcal{T}(\mathbf{X})$, and FORM then searches for the design point \mathbf{z}^* in the standard normal space. Classically, the Nataf transform is used to perform the mapping, under the implicit assumption that $F_{\mathbf{X}}$ has a Gaussian copula Der Kiureghian and Liu (1986). To generalise the approach to non-Gaussian dependence structures, we propose to express $F_{\mathbf{X}}$

in terms of its marginals F_i and its copula $C_{\mathbf{X}}$ as in (1), and to model $C_{\mathbf{X}}$ as an R-vine (see Section 2.4), whose Rosenblatt transform can be computed (see Section 3.3).

4.4 Importance sampling

Importance sampling (IS) is designed to combine the convergence speed of FORM with the robustness of MC sampling. For a general, non-standard-normal \mathbf{X} with Rosenblatt transform $\mathbf{Z} = \mathcal{T}^{(\mathcal{N})}(\mathbf{X})$, (28) can be recast as

$$P_f = \int_{\mathbb{R}^M} \mathbf{1}_{\mathcal{D}_f}(\mathcal{T}^{-1}(\mathbf{z})) \frac{\varphi_M(\mathbf{z})}{\psi(\mathbf{z})} \psi(\mathbf{z}) d\mathbf{z} = \mu_\psi \left(\mathbf{1}_{\mathcal{D}_f}(\mathcal{T}^{-1}(\mathbf{Z})) \frac{\varphi_M(\mathbf{Z})}{\psi(\mathbf{Z})} \right), \quad (29)$$

where $\varphi_M(\cdot)$ is the M-variate standard normal density, $\psi(\cdot)$ is a suitable M-variate density (the *importance density*) and μ_ψ is the mean operator with respect to ψ . Melchers (1999) recommends to assign ψ as the standard normal density centered at the design point found by FORM: $\psi(\mathbf{z}) = \varphi_M(\mathbf{z} - \mathbf{z}^*)$.

Given a sample $\{\hat{\mathbf{z}}^{(1)}, \dots, \hat{\mathbf{z}}^{(n)}\}$ of $\psi(\mathbf{Z})$, the IS estimator of P_f is the sample estimator

$$\hat{P}_{f;\text{IS}} = \frac{1}{N} \exp(\|\mathbf{z}^*\|^2/2) \sum_{j=1}^n \mathbf{1}_{\mathcal{D}_f}(\mathcal{T}^{-1}(\hat{\mathbf{z}}^{(j)})) \exp(-\hat{\mathbf{z}}^{(j)} \cdot \mathbf{z}^*),$$

which has variance

$$\sigma^2(\hat{P}_{f;\text{IS}}) \approx \frac{1}{n(n-1)} \sum_{j=1}^n \left(\mathbf{1}_{\mathcal{D}_f}(\mathcal{T}^{-1}(\hat{\mathbf{z}}^{(j)})) \frac{\varphi_M(\hat{\mathbf{z}}^{(j)})}{\varphi_M(\hat{\mathbf{z}}^{(j)} - \mathbf{z}^*)} - \hat{P}_{f;\text{IS}} \right)^2$$

and $\text{CoV}(\hat{P}_{f;\text{IS}}) \approx \sigma(\hat{P}_{f;\text{IS}})/\hat{P}_{f;\text{IS}}$. Since the latter is given in terms of $\hat{P}_{f;\text{IS}}$, it is unknown until $\hat{P}_{f;\text{IS}}$ is computed. One can progressively increase the sample size n until $\text{CoV}(\hat{P}_{f;\text{IS}})$ drops below a desired level.

5 Results on a horizontal truss model

We first demonstrated the analysis workflow developed above on a horizontal truss model. Estimates based on advanced and computationally efficient UQ techniques were compared to reference MCS estimates. The analysis was run in Matlab (Mat, 2016). Specifically, the vine copula representation and fitting procedure were performed using the open source package VineCopulaMatlab (Kurz, 2015). We enriched this toolbox with a few functionalities for the computation of the Rosenblatt and inverse Rosenblatt transforms of C- and D- vines, and for the calculation of the optimal D-vine structure on data, implemented as an open travelling salesman problem (Applegate et al., 2006). The UQ analyses were performed with the free Matlab-based software UQLAB (Marelli and Sudret, 2014).

5.1 Computational model

The horizontal truss model, already used in Blatman and Sudret (2011), comprises 23 bars connected at 6 upper nodes, as shown in Figure 2. The structure is 24 meters long and 2

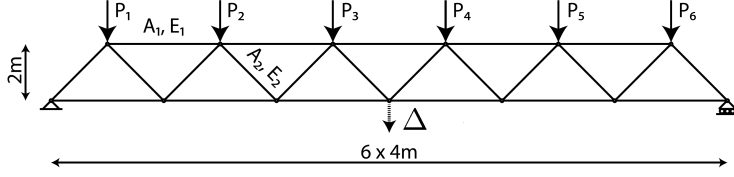


Figure 2: **Scheme of the horizontal truss model.** Modified from Blatman and Sudret (2011).

meters high. Six random loads P_1, P_2, \dots, P_6 were applied onto the structure, one on each upper node. As a result, the structure exhibited a downward vertical displacement at each node. The largest displacement Δ was always at the center. Excess displacement leads to failure.

5.2 Probabilistic input model

We considered the case of uncertain loads P_i , causing uncertainty in the output response Δ . The bar properties of the truss, differently from Blatman and Sudret (2011), were kept constant. The loads $\mathbf{X} = (P_1, P_2, \dots, P_6)$ were modelled by assigning separately their marginals F_i and their copula $C_{\mathbf{X}}$. We fixed the marginals to univariate Gumbel CDFs with mean $\mu = 5 \times 10^4$ N and standard deviation $\sigma = 0.15\mu = 7.5 \times 10^3$ N:

$$F_i(x; \alpha, \beta) = e^{-e^{-(x-\alpha)/\beta}}, \quad x \in \mathbb{R}, i = 1, 2, \dots, 6, \quad (30)$$

where $\beta = \sqrt{6}\sigma/\pi$, $\alpha = \mu - \gamma\beta$, and $\gamma \approx 0.5772$ is the Euler-Mascheroni constant.

We then investigated how different copulas affect the statistics of the truss response. First, we employed the independence copula $C^{(\Pi)}$ defined by (11), which implies independence among the loads.

Loads on a truss structure may be expected to be positively correlated: higher loads on one node increase the chance to have higher loads on other nodes (e.g. due to snow or traffic jam on a bridge). To account for this, we selected next a 6-dimensional Gaussian copula $C^{(\mathcal{N})}$ (12). We assigned the copula parameters ρ_{1j} , $j = 2, \dots, 6$, such that the Spearman's correlation coefficients (6) would be $\rho_{S;1j} = 0.135$, resulting in $\rho_{1j} = 0.141$ (and Kendall's tau $\tau_{K;1j} \simeq 0.0904$). Besides, we set $\rho_{S;i;j|1} = 0$ for each $i \neq j$, $i, j \neq 1$, so that all loads other than P_1 would be conditionally independent given P_1 .

Beside being positively correlated, in a realistic scenario loads are likely to be upper tail dependent: an extremely large load on one node increases the chance to have large loads elsewhere (e.g., when due to a heavy snowfall or to a traffic jam). Therefore, we last investigated a scenario with tail dependent loads (see Section 2.2). We modelled upper tail dependence by means of a C-vine $C^{(\mathcal{V})}$. We selected P_1 as the first node of $C^{(\mathcal{V})}$, and we set the pair copulas in the first tree to bivariate Gumbel-Hougaard copulas $C_{1j}^{(\mathcal{GH})}$ (13) between

P_1 and P_j , $j = 2, \dots, 5$. We took the parameter $\theta_{1j} = 1.1$, $j = 2, \dots, 6$, yielding Spearman's correlation coefficients $\rho_{S;1j} = 0.135$ as for the Gaussian copula. This choice resulted in $\tau_{K;1j} = 0.0909$ (close to the value determined by the Gaussian copula) but also determined an upper tail dependence coefficient $\lambda_{u;1,j} = 0.122$ between P_1 and P_j . We further set the other pair copulas of the vine, *i.e.*, all conditional pair copulas, to the independence copula, ensuring conditional independence of (P_i, P_j) given P_1 for each $i, j \neq 1$. The resulting vine was

$$C^{(\mathcal{V})}(u_1, \dots, u_6) = \prod_{j=2}^6 C_{1j}^{(\mathcal{GH})}(u_1, u_j). \quad (31)$$

Note that other vine structures could have been used to model tail dependent loads: for instance, a D-vine whose first tree couples the loads on neighbouring nodes of the truss. Expert knowledge and available input data usually provide guidance in this selection process, as discussed in Section 2.5.

To demonstrate the viability of the vine representation in cases where the vine itself is not known and has to be inferred from data, we finally replaced the parameter values θ_{ij} of $C^{(\mathcal{V})}$ with their maximum likelihood estimates based on $m = 300$ observations sampled from $C^{(\mathcal{V})}$. In real applications, these observations (of the input only) could be obtained by monitoring of the loads themselves, or estimated from available data (*e.g.*, weather or traffic conditions), and do not require any model evaluation. The resulting C-vine $\hat{C}^{(\mathcal{V})}$ had parameters

$$\hat{\theta}_{12} = 1.096, \hat{\theta}_{13} = 1.112, \hat{\theta}_{14} = 1.133, \hat{\theta}_{15} = 1.075, \hat{\theta}_{16} = 1.125.$$

All conditional pair copulas were correctly found to be independence copulas.

5.3 Analysis of the moments for different load couplings

For each probabilistic model of the loads, we analysed the mean $\mu(\Delta)$ and standard deviation $\sigma(\Delta)$ of the resulting system response by MCS and by PCE.

The MC estimates were computed as sample estimates on $\{\hat{\delta}_i = \mathcal{M}(\hat{\mathbf{x}}_i)\}_{i=1}^{10^7}$, where $\{\hat{\mathbf{x}}_i\}_{i=1}^{10^7}$ were i.i.d realisations of the input, obtained by Sobol sampling. The δ_i were computationally affordable to compute due to the simplicity of the model. The results are summarised in Table 2, together with the CoV of the estimates (see Table 1).

While $\mu(\Delta)$ was virtually identical across the input model, $\sigma(\Delta)$ exhibited non-negligible changes. Importantly, it increased by about 3% from the Gaussian to the vine copula, despite the means, variances and Spearman's correlation coefficients of the loads being identical across the two probabilistic models. As a consequence, if $C^{(\mathcal{V})}$ were the true copula among the loads, an MCS estimate of $\sigma(\Delta)$ based on the Gaussian assumption would be biased. Conversely, fitting $C^{(\mathcal{V})}$ to data yielded more precise estimates.

MC estimates converge slowly and therefore need to be computed on large samples. Figure 3 shows by solid lines the errors on MC estimates drawn for the four different copulas

	$C^{(\text{II})}$	$C^{(\mathcal{N})}$	$C^{(\mathcal{V})}$	$\hat{C}^{(\mathcal{V})}$
$\hat{\mu}_{\text{MC}}(\Delta)$ (cm):	$\hat{\mu}_{\text{MC}}^{(\text{II})} = 7.78$	$\hat{\mu}_{\text{MC}}^{(\mathcal{N})} = 7.78$	$\hat{\mu}_{\text{MC}}^{(\mathcal{V})} = \mathbf{7.78}$	$\hat{\mu}_{\text{MC}}^{(\hat{\mathcal{V}})} = 7.78$
$\text{CoV}(\hat{\mu}_{\text{MC}}(\Delta)) (\times 10^{-5})$:	2.1	2.3	2.4	2.4
$\hat{\sigma}_{\text{MC}}(\Delta)$ (cm):	$\hat{\sigma}_{\text{MC}}^{(\text{II})} = 0.528$	$\hat{\sigma}_{\text{MC}}^{(\mathcal{N})} = 0.566$	$\hat{\sigma}_{\text{MC}}^{(\mathcal{V})} = \mathbf{0.581}$	$\hat{\sigma}_{\text{MC}}^{(\hat{\mathcal{V}})} = 0.585$
$\text{CoV}(\hat{\sigma}_{\text{MC}}(\Delta)) (\times 10^{-4})$:	2.2	2.2	2.2	2.2

Table 2: **Moments of truss deflection for different load couplings.** MC estimates $\hat{\mu}_{\text{MC}}(\Delta)$ and $\hat{\sigma}_{\text{MC}}(\Delta)$ for different copulas of the loads, based on 10^7 samples, and their CoV. Reference solutions in bold.

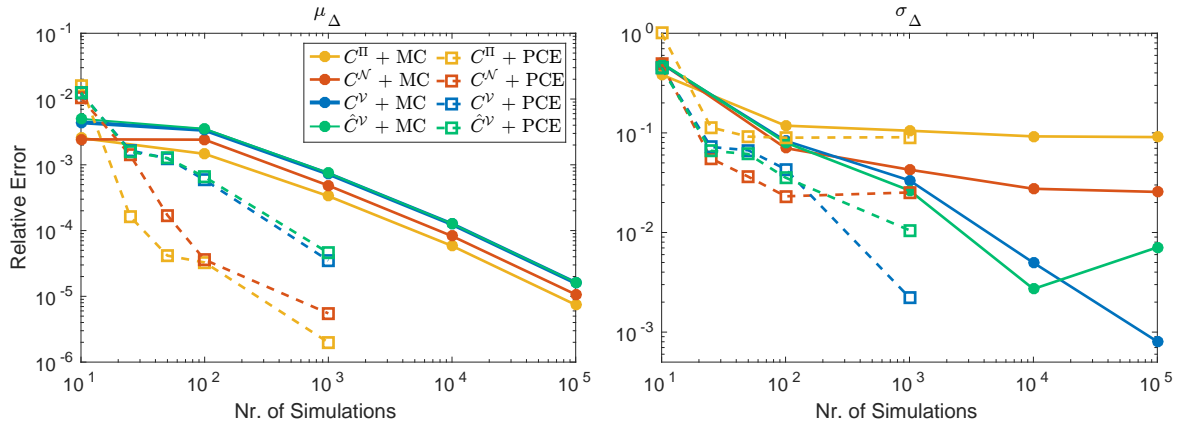


Figure 3: **Estimates of the deflection moments.** Estimates of the errors on $\mu(\Delta)$ (left panel) and on $\sigma(\Delta)$ (right panel) obtained using an increasing number of samples by MCS (solid lines) and by PCE (dashed lines), for loads coupled by $C^{(\text{II})}$ (yellow), $C^{(\mathcal{N})}$ (red), $C^{(\mathcal{V})}$ (blue) and $\hat{C}^{(\mathcal{V})}$ (green). Reference solution: MC estimate obtained on 10^7 samples with copula $C^{(\mathcal{V})}$.

on $10, 100, \dots, 10^5$ samples. The reference solutions were the MC estimates $\hat{\mu}_{\text{MC}}^{(\mathcal{V})}$, $\hat{\sigma}_{\text{MC}}^{(\mathcal{V})}$ obtained through 10^7 samples under $C^{(\mathcal{V})}$. The errors of estimates $\tilde{\mu}$, $\tilde{\sigma}$ were defined as

$$E_{\text{rel}}^{(\mu)} = \left| \frac{\tilde{\mu}}{\hat{\mu}_{\text{MC}}^{(\mathcal{V})}} - 1 \right|, \quad E_{\text{rel}}^{(\sigma)} = \left| \frac{\tilde{\sigma}}{\hat{\sigma}_{\text{MC}}^{(\mathcal{V})}} - 1 \right|. \quad (32)$$

Note that, due to the CoV of the reference solutions (see Table 2), the errors shown in Figure 3 are reliable only down to approximately 10^{-4} for the means and 10^{-3} for the standard deviations.

We further estimated for each copula the error on $\mu(\Delta)$ and $\sigma(\Delta)$ yielded by PCE, which is known to converge faster than MCS (see Section 4.2). We increased the size of the experimental design from 10 to 1000 sample points. The errors on the PCE estimates are shown in Figure 3 by dashed lines (again, reliable only down to the above mentioned precision). Notably, for the same number n of samples the PCE error is significantly smaller

Method:	MCS				FORM			
	$C^{(\Pi)}$	$C^{(\mathcal{N})}$	$C^{(\mathcal{V})}$	$\hat{C}^{(\mathcal{V})}$	$C^{(\Pi)}$	$C^{(\mathcal{N})}$	$C^{(\mathcal{V})}$	$\hat{C}^{(\mathcal{V})}$
Copula:								
\hat{P}_f ($\times 10^{-4}$):	0.15 ± 0.01	0.34 ± 0.02	5.04 ± 0.07	5.71 ± 0.08	0.037	0.10	4.88	5.44
CoV(\hat{P}_f) (%):	8.2	5.4	1.4	1.3	–	–	–	–
# runs:	10^7	10^7	10^7	10^7	219	219	108	128

Table 3: **Estimates of the truss failure probability.** Estimates of P_f obtained with different copulas and methods (for MCS with standard deviation of the estimator; reference solution in bold), CoV of the MC estimate (see Table 1), and number of runs of the computational model needed to obtain the solution.

than the MCS error, demonstrating that the vine representation is fully compatible with PCE metamodeling.

5.4 Reliability analysis for different load couplings

The truss model was set to fail if the deflection Δ reached or exceeded the critical threshold $\delta^* = 11$ cm. Reliability analysis was performed to evaluate the failure probability $P_f = \mathbb{P}(\Delta \geq \delta^*) = 1 - F_{\Delta}(\delta^*)$.

For each probabilistic input model (i.e. for each copula $C_{\mathbf{X}}$, combined with the marginals in (30)), we first obtained reference solutions by MCS. We drew $n = 10^7$ i.i.d realisations $\{\hat{\mathbf{x}}_i\}_{i=1}^{10^7}$ of the input by Sobol sampling, we computed the corresponding deflections $\{\hat{\delta}_i = \mathcal{M}(\hat{\mathbf{x}}_i)\}_{i=1}^{10^7}$, and estimated P_f as the fraction of observed deflections larger than 11 cm. Then, we drew estimates by FORM, applied on the compositional model resulting from decoupling the loads via Rosenblatt transformation (see Section 3). The results are summarised in Table 3.

The failure probability estimated by MCS with the independence copula $C^{(\Pi)}$ was $\hat{P}_f^{(\Pi)} = (1.5 \pm 0.1) \times 10^{-5}$. The FORM estimate was $\hat{P}_{f;\text{FORM}}^{(\Pi)} = 0.37 \times 10^{-5}$, obtained by 219 runs of the computational model. Figure 4B shows, in yellow, the empirical survival function of Δ obtained under $C^{(\Pi)}$, for values of δ ranging from 6 cm to 12 cm. The vertical dashed line marks the critical threshold δ^* , whereas the square indicates the FORM estimate of P_f .

The MC estimate of P_f under the Gaussian copula $C^{(\mathcal{N})}$ was $\hat{P}_{f;\text{MC}}^{(\mathcal{N})} = (3.4 \pm 0.2) \times 10^{-5}$ (Figure 4, orange line: empirical survival function of Δ under $C^{(\mathcal{N})}$). Compared to the independent case, the failure probability increased by a factor of over 2, as a result of the positive correlations among the loads. The FORM estimate was $\hat{P}_{f;\text{FORM}}^{(\mathcal{N})} = 1.0 \times 10^{-5}$, obtained again by 219 runs.

The MC estimate of P_f under the C-vine $C^{(\mathcal{V})}$ was $\hat{P}_{f;\text{MC}}^{(\mathcal{V})} = (5.04 \pm 0.07) \times 10^{-4}$ (Figure 4, blue line: empirical survival function of Δ under $C^{(\mathcal{V})}$). This value was over 33 times larger than the case of independent loads and 14 times larger than the Gaussian case, despite

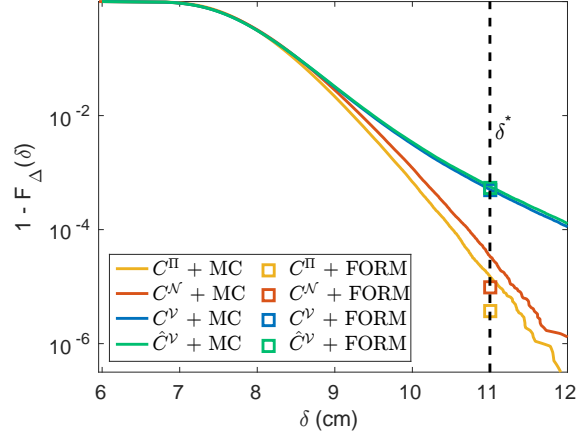


Figure 4: **Reliability analysis of the truss structure.** Solid lines: MC estimate of the survival function $\mathbb{P}(\Delta > \delta)$ for loads coupled by the independence copula $C^{(\Pi)}$ (yellow), the Gaussian copula $C^{(\mathcal{N})}$ (red), the C-vine with known parameters $C^{(\mathcal{V})}$ (blue, mostly overlapping with green), and the C-vine with fitted parameters $\hat{C}^{(\mathcal{V})}$ (green). The vertical dashed line marks the critical threshold δ^* . Squares: estimates of P_f obtained by FORM.

the marginal distributions of the loads being identical across all cases, and the correlation matrix \mathbf{R} being identical between $C^{(\mathcal{V})}$ and $C^{(\mathcal{N})}$. The FORM estimate using $C^{(\mathcal{V})}$ was $\hat{P}_{f;\text{FORM}}^{(\mathcal{V})} = 4.88 \times 10^{-4}$, obtained by only 108 runs.

Finally, the MC estimate of P_f assuming $\hat{C}^{(\mathcal{V})}$ was $\hat{P}_{f;\text{MC}}^{(\hat{\mathcal{V}})} = 5.52 \times 10^{-4}$, only 9.5% larger than the reference solution $\hat{P}_{f;\text{MC}}^{(\mathcal{V})}$ (Figure 4, green line: empirical survival function of Δ under $\hat{C}^{(\mathcal{V})}$). The FORM estimate, obtained with 128 runs of the computational model, was $\hat{P}_{f;\text{FORM}}^{(\hat{\mathcal{V}})} = 5.44 \times 10^{-4}$ (8% larger than $\hat{P}_{f;\text{MC}}^{(\mathcal{V})}$).

In light of these results, in a scenario where the true dependence among the loads is described by (31), assuming independence or a Gaussian copula among the loads (as, *e.g.*, done when using the Nataf transform) would cause a severe underestimation of the failure probability of the system, even when relying on a large MCS strategy. Properly capturing the dependencies among the inputs is thus more critical towards getting accurate estimates of P_f than using more efficient estimation algorithms (FORM combined with $C^{(\mathcal{V})}$ outperforms MCS on 10^7 samples combined with $C^{(\mathcal{N})}$). Furthermore, the error remains small when the vine is inferred from available data, demonstrating the viability of the vine copula modelling framework in reliability analysis for purely data driven inference.

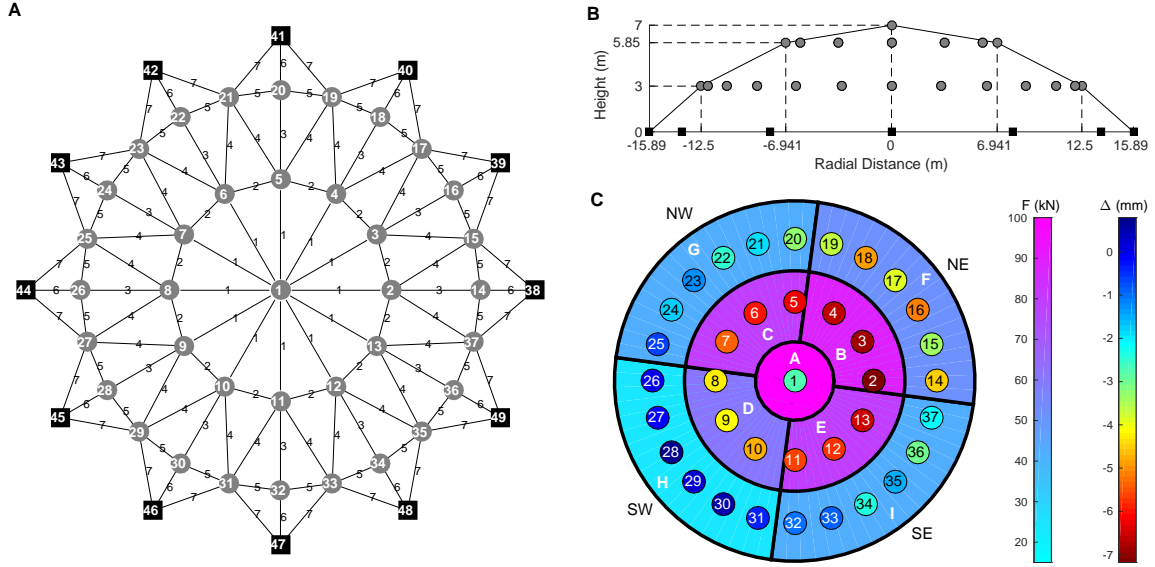


Figure 5: **Dome structure and average response to loads.** **A)** Truss model, consisting of 37 central nodes (grey dots, 1-37), 12 support nodes (black squares, 37-49) and 120 bars connecting them, divided into 7 groups. **B)** Profile of the dome with spatial dimensions. **C)** Sectors of the dome surface and nodes in each sector. The color of each sector represents the total average load weighing on each node in the sector (left color bar). The color of each node marks the average vertical displacement of that node in response to the loading, calculated over 250 Monte-Carlo simulations.

6 Results on a dome truss model under asymmetric loads

We further considered a more complex model of a three-dimensional 120-bar dome truss. The model was used to demonstrate the applicability of our novel copula-based UQ framework on a more realistic case study than the one previously analysed. Due to the computational complexity of this model (~ 15 seconds/run), large MCS was not affordable.

6.1 Computational model

The dome structure, illustrated in Figure 5A from the top and Figure 5B from the front, consists of 120 bars connected to a total of 49 nodes. Nodes 1 to 37 (grey dots) are unsupported and therefore, when subject to vertical loading, exhibit a displacement from the original position in possibly all three directions. The dimensions of the structure are reported in panel B.

The computational model was implemented in the finite element software Abaqus Smith (2009). This structure was previously analysed in Kaveh and Talatahari (2009) to obtain

Group:	Optimal cross-sectional areas (cm ²)							Weight (kN)	Loads (kN)			
	1	2	3	4	5	6	7		Node:	1	2-13	14-37
Area:	24.38	21.79	26.61	17.64	10.38	22.79	16.38	89.35	Load:	60	30	10

Table 4: **Dome’s structural parameters and loads.** Cross-section of each group of bars that minimises the total structural weight under stress and x -, y - displacement constraints, resulting structural weight, and additional loads on each node. Values provided by Kaveh and Talatahari (2009).

optimal sizing variables so as to minimise the total structural weight. The authors distinguished 7 groups of bars, and optimised the cross-sections of each group to minimise the total structural weight of the structure under 4 different types of stress and displacement constraints. We considered in particular their case 2, where stress and displacement constraints (± 5 mm) in the x - and y - directions were enforced. In Kaveh and Talatahari (2009) it was further assumed that each unsupported node is subject to vertical loading, taken as 60 kN at node 1, 30 kN at nodes 2-14, and 10 kN at nodes 15–37. Under these conditions, the optimal cross sections reported in Table 4 were obtained, yielding a total structural weight of 89,35 kN.

6.2 Probabilistic input model

Here we were interested in analysing the displacement of the nodes, considered as a risk factor potentially leading to failure.

First, we assigned uncertainty to the bar cross-sections. We modelled the 7 previously identified groups by independent log-normal random variables with mean given by the values in Table 4 and CoV $\sigma/\mu = 0.03$. We assigned the bars in each of the 7 groups identical cross-sections.

We further assigned uncertainty to the loads applied on each node. We modelled a scenario where loads are distributed asymmetrically over the structure. A preliminary analysis showed that asymmetric loads yielded higher maximum vertical displacement compared to symmetric loads. We divided the 37 central nodes into 9 groups, named A to I, corresponding to different sectors of the surface of the dome. Sector A contains solely node 1, sector B contains nodes 2, 3 and 4, and so on, as shown in Figure 5 and in the upper two rows of Table 5. We considered the nodes in each group to be subject to the same load, and modelled the loads on the 9 groups by a 9-dimensional random vector with prescribed marginals and copula. The marginals were taken to be Gumbel distributions (30), whose moments, shown in the bottom two rows of Table 5, were determined as follows. We assigned to each sector a Gumbel-distributed load, having mean 1 kN/m² for the top and north-east sectors

Sector		A	B	C	D	E	F	G	H	I
Nodes		1	2-4	5-7	8-10	11-13	14-19	20-25	26-31	32-37
$L_{\text{fix}}/\text{Node}$ (kN)		60	30 each				10 each			
Sector's Area (m ²)		37.84	257.00 each				496.38 each			
Area/Node (m ²)		37.84	86.33 each				82.73 each			
$L_{\text{ext}}/\text{m}^2$ (kN)		1	1	0.5	0.25	0.5	1	0.5	0.25	0.5
$\mu(L_{\text{ext}}/\text{Node})$ (kN)		37.84	21.58	10.79	5.40	10.79	20.68	10.34	5.17	10.34
$\mu(L_{\text{tot}}/\text{Node})$ (kN)		97.84	51.58	40.79	35.40	40.79	30.68	20.34	15.17	20.34
$\sigma(L_{\text{tot}}/\text{Node})$ (kN)		7.57	4.32	2.16	1.08	2.16	4.14	2.07	1.03	2.07

Table 5: **Load statistics on each dome sector.** For each node sector from A to I: nodes in the sector, structural load L_{fix} per node, average external load L_{ext} per node, moments of the total load L_{tot} .

A,B,F, 0.5 kN/m² for the north-west and south-east sectors C, E, G and I, and 0.25 kN/m² for the south-west sectors D and H. The different mean values could model, for instance, snow falling on the dome from the north-east direction. The average external weight on each node (third-last row of the table) was obtained by multiplication with the total area of the node's sector (fourth row) and by division with the number of nodes in that sector. The CoV of each distribution was set to 0.2. Finally, deterministic service loads similar to those suggested by Kaveh and Talatahari (2009) were added: 60 kN on node 1, 30 kN on nodes 2-13, 10 kN on nodes 14 – 37.

We coupled the 9 loads by three different copulas: the independence copula $C^{(\Pi)}$ (11), the Gaussian copula $C^{(\mathcal{N})}$ (12), and a 9-dimensional C-vine $C^{(\mathcal{V})}$ (31).

The C-Vine consisted of Gumbel-Hougaard pair-copulas (13), each with parameter $\theta = 5$, between sector A and sectors B, \dots, I for the first tree, and independence conditional pair-copulas for the other trees. This choice assigns the loads between nodes in sector A and any other loads a Kendall's correlation coefficient $\tau_K = 0.8$ and an upper tail dependence coefficient $\lambda_u = 0.85$. Thus, $C^{\mathcal{V}}$ assigns a strong positive correlation to the loads and a high probability of having joint extremes if one of the loads takes values in its upper tail. The Gaussian copula was taken such that its correlation matrix would match the correlation coefficients determined by the C-Vine.

We further built a C-vine fitted on 300 samples from $C^{(\mathcal{V})}$. The resulting vine $\hat{C}^{(\mathcal{V})}$ had the same structure as $C^{(\mathcal{V})}$, and Gumbel-Hougaard copulas $C_{AB}, C_{AC}, \dots, C_{AI}$ with parameters

$$\begin{aligned} \theta_{AB} &= 5.09, \theta_{AC} = 4.84, \theta_{AD} = 5.15, \theta_{AE} = 4.78, \\ \theta_{AF} &= 4.63, \theta_{AG} = 5.02, \theta_{AH} = 4.71, \theta_{AI} = 5.02. \end{aligned}$$

	$C^{(\Pi)}$	$C^{(\mathcal{N})}$	$C^{(\mathcal{V})}$	$\hat{C}^{(\mathcal{V})}$
$\hat{\mu}_{\text{PCE}}(\Delta)$ (mm):	$\hat{\mu}_{\text{PCE}}^{(\Pi)} = -7.193$	$\hat{\mu}_{\text{PCE}}^{(\mathcal{N})} = -7.183$	$\hat{\mu}_{\text{PCE}}^{(\mathcal{V})} = \mathbf{-7.182}$	$\hat{\mu}_{\text{PCE}}^{(\hat{\mathcal{V}})} = -7.183$
$\hat{\sigma}_{\text{PCE}}(\Delta)$ (mm):	$\hat{\sigma}_{\text{PCE}}^{(\Pi)} = 1.164$	$\hat{\sigma}_{\text{PCE}}^{(\mathcal{N})} = 0.588$	$\hat{\sigma}_{\text{PCE}}^{(\mathcal{V})} = \mathbf{0.552}$	$\hat{\sigma}_{\text{PCE}}^{(\hat{\mathcal{V}})} = 0.556$

Table 6: **Moments of truss response for different load couplings.** Monte Carlo estimates of $\mu(\Delta)$ and $\sigma(\Delta)$ for different copulas of the loads, based on 10^7 samples, and their CoV. Reference solutions in bold.

6.3 Model response to the uncertain input

The output of the model in response to a single instance of the input is a list of displacements in the x -, y - and z - directions, one per node, as well as the tension (or compression) of each bar. We restricted our attention to displacements only, which, if excessive, may lead to failure of the structure.

We first performed a preliminary Monte-Carlo analysis based on 250 simulations of the input (with loads coupled by $C^{\mathcal{V}}$) and corresponding output displacements. Figure 5C shows in two different color codes the average weights on the nodes in each sector (left color bar) and the resulting average vertical displacement of each node (right color bar). Negative displacement indicates that the node moved downwards. Some nodes exhibited positive displacements, *i.e.*, uplifting.

For all simulations and all nodes, the vertical displacement always exceeded in absolute value the displacement in the x - and y - directions. This was expected, considering that the average bar's cross-sections were optimised to minimise the latter. Besides, the absolute vertical displacement was always maximal at node 2. Thus, we reduced the model's response to the vertical displacement Δ of node 2:

$$\Delta = \mathcal{M}(\mathbf{X}), \quad \mathbf{X} = (A_1, \dots, A_7, L_A, \dots, L_I).$$

6.4 Analysis of the moments

For each copula mentioned above, we evaluated the mean $\mu(\Delta)$ and the standard deviation $\sigma(\Delta)$ of the deflection Δ at node 2 both by MCS and by PCE. The estimates were based on samples of size n increasing from 10 to 1000. Due to the generally faster convergence of PCE with respect to MCS for small sample sizes, the PCE estimates built on 1000 samples were taken as reference values for each of the four copula models (see Table 6). The obtained values indicate that the independence, Gaussian and vine copulas yielded for Δ similar means but different standard deviations.

Taken in particular $C^{(\mathcal{V})}$ to be the true copula among the loads, and the corresponding PCE estimates $\hat{\mu}_{\text{PCE}}^{(\mathcal{V})}$ and $\hat{\sigma}_{\text{PCE}}^{(\mathcal{V})}$ based on 1000 points to be the reference solutions, we com-

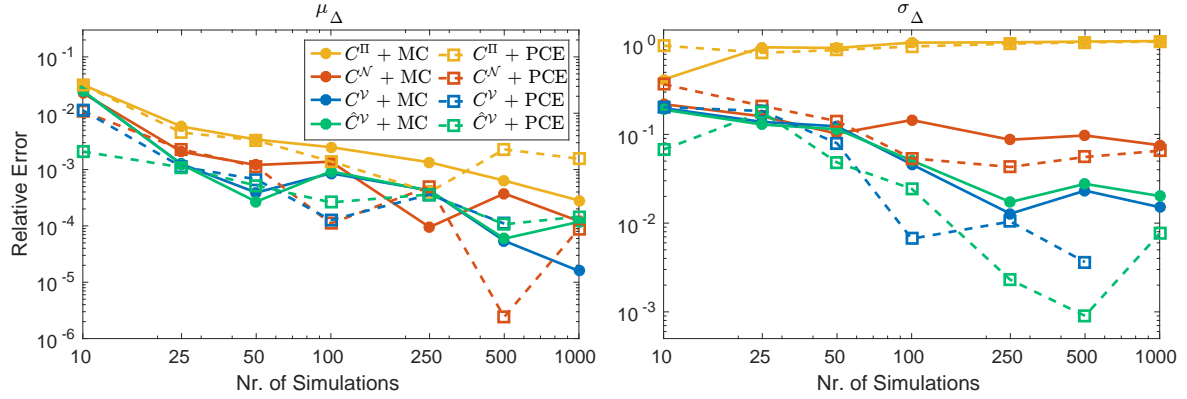


Figure 6: **Moments of dome's deflection Δ** . Estimates of the errors on $\mu(\Delta)$ (left panel) and on $\sigma(\Delta)$ (right panel) obtained using an increasing number of samples by MCS (solid lines) and by PCE (dashed lines), for loads coupled by $C^{(\text{II})}$ (yellow), $C^{(\mathcal{N})}$ (red), $C^{(\mathcal{V})}$ (blue) and $\hat{C}^{(\mathcal{V})}$ (green). Reference solutions: PCE estimates $\tilde{\mu}^{(\mathcal{V})}$, $\tilde{\sigma}^{(\mathcal{V})}$ obtained on 1000 samples with copula $C^{(\mathcal{V})}$.

puted the relative error of all other estimates. The errors, defined analogously to (32), are shown in Figure 6. From these results, three main conclusions can be drawn. First, if $C^{(\mathcal{V})}$ was the true copula among the loads, neither $C^{(\text{II})}$ nor $C^{(\mathcal{N})}$ would offer adequate alternative representations, since the associated standard deviations differ by 111% and 6.5% from their reference value, respectively. Second, employing the fitted vine $\hat{C}^{(\mathcal{V})}$ in combination with MCS (green solid line) allows one to approximate the moments with higher precision than the Gaussian (red) or independence (yellow) copulas. Finally, PCE combines well with the vine representation (dashed lines), yielding the smallest errors. It is worth noting, however, that using a proper copula model (a vine instead of a Gaussian or independence copula) is more important to obtain accurate estimates (particularly for $\sigma(\Delta)$) than using a more advanced UQ method (PCE instead of MC).

6.5 Reliability analysis

The dome structure was further set to fail if the displacement Δ was equal to or lower than the critical threshold $\delta^* = -11$ mm. We performed reliability analysis to estimate the failure probability $P_f = \mathbb{P}(\Delta \leq \delta^*) = F_\Delta(\delta^*)$ of excessive downward vertical displacement.

We performed 5000 simulations by MCS for each copula of the input model, keeping the marginals identical across the models. Figure 7 shows the CDFs resulting from copulas $C^{(\mathcal{V})}$ (blue), $\hat{C}^{(\mathcal{V})}$ (green), $C^{(\mathcal{N})}$ (red), and $C^{(\text{II})}$ (yellow), evaluated for probabilities down to 10^{-3} .

The MC estimate of P_f under $C^{(\text{II})}$ was $\hat{P}_{f;\text{MC}}^{(\text{II})} = (6.8 \pm 1.2) \times 10^{-3}$. For copulas $C^{(\mathcal{N})}$, $C^{(\mathcal{V})}$ and $\hat{C}^{(\mathcal{V})}$ no simulations led to values of Δ below δ^* . We then resorted to FORM to evaluate P_f for each copula, obtaining the estimates $\hat{P}_{f;\text{FORM}}^{(\text{II})} = 8.0 \times 10^{-3}$, $\hat{P}_{f;\text{FORM}}^{(\mathcal{N})} =$

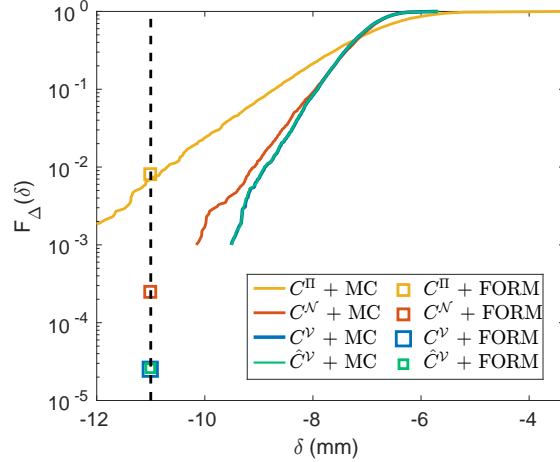


Figure 7: **Dome failure probability.** The solid lines show the MC estimates of the response CDF $F_{\Delta}(\delta) = \mathbb{P}(\Delta \leq \delta)$ (for values down to 10^{-3}) under loads coupled by $C^{(II)}$ (yellow), $C^{(N)}$ (red), $C^{(V)}$ (blue) and $\hat{C}^{(V)}$ (green). The vertical dashed line represents the critical threshold δ^* . The markers on it indicate the FORM estimates obtained for each copula model.

Method:	MCS				FORM				IS			
	$C^{(II)}$	$C^{(N)}$	$C^{(V)}$	$\hat{C}^{(V)}$	$C^{(II)}$	$C^{(N)}$	$C^{(V)}$	$\hat{C}^{(V)}$	$C^{(II)}$	$C^{(N)}$	$C^{(V)}$	$\hat{C}^{(V)}$
$\hat{P}_f (\times 10^{-5})$:	680 ± 120	–	–	–	800	25	2.53	2.56	713 ± 70	24.7 ± 2.4	3.13 ± 0.29	3.21 ± 0.30
CoV(\hat{P}_f) (%)	17.6	–	–	–	–	–	–	–	9.9	9.9	9.3	9.3
tot. # runs:	5000	5000	5000	5000	182	349	276	181	482	749	876	781

Table 7: **Estimates of the dome failure probability.** Estimates of P_f obtained with different copulas and methods (reference solution in bold), CoV of the MC and IS estimates, and number of runs needed for the estimation.

2.50×10^{-4} , $\hat{P}_{f;\text{FORM}}^{(V)} = 2.53 \times 10^{-5}$, and $\hat{P}_{f;\text{FORM}}^{(\hat{V})} = 2.54 \times 10^{-5}$. Since MC estimates were not available or not reliable here, we further performed IS to improve the FORM estimates and to get confidence intervals (see Section 4.4). We increased the IS sample size in steps of 100, until the CoV of the estimate was lower than 10%. We obtained the estimates $\hat{P}_{f;\text{IS}}^{(II)} = (7.13 \pm 0.70) \times 10^{-3}$, $\hat{P}_{f;\text{IS}}^{(N)} = (2.47 \pm 0.24) \times 10^{-4}$, $\hat{P}_{f;\text{IS}}^{(V)} = (3.13 \pm 0.29) \times 10^{-5}$, and $\hat{P}_{f;\text{IS}}^{(\hat{V})} = (3.21 \pm 0.30) \times 10^{-5}$.

The results, summarized in Table 7, show that the failure probability of the structure decreases by an order of magnitude from $C^{(II)}$ to $C^{(N)}$, and by another order of magnitude from $C^{(N)}$ to $C^{(V)}$ and $\hat{C}^{(V)}$. Highly asymmetric loads (as due to $C^{(II)}$ and, to a minor extent, to $C^{(N)}$) may create a deformation mechanism in the structure that favours large displacements of the most heavily loaded nodes (here, node 2). In contrast, the more symmetric loading determined by the C-vine results in a more evenly distributed load path that

ultimately leads to a safer structure. If the loads were actually coupled by $C^{(\nu)}$, assuming the independence or Gaussian copulas would thus lead to highly overestimating P_f . Conversely, fitting $C^{(\nu)}$ to data would recover the reference solution $\hat{P}_{f;IS}^{(\nu)}$ with high precision. Again, the input model used for the analysis is more important to get an accurate estimate than the particular UQ method (FORM, IS) employed.

7 Discussion

We proposed a general framework that enables uncertainty quantification (UQ) for problems where the input parameters of the system exhibit complex, non-Gaussian dependencies (copulas). The joint CDF of input parameters is expressed in terms of marginals and a copula, which are modelled separately. The copula is further modelled as a vine copula, *i.e.*, a product of simpler 2-copulas. This specification eases its construction, especially in high dimension, and offers a simple interpretation of the dependence model. A wide range of different dependence structures can be modelled using this approach.

Our framework focuses in particular on regular (R-) vines, for which algorithms exist to compute the likelihood on available data, thus enabling parameter fitting. In addition, R-vines offer algorithms to compute the associated Rosenblatt transform and its inverse on data, needed to map the original input random vector into a vector with independent components and back. Thus, UQ techniques that work for independent inputs can be applied to any inputs coupled by R-vines. In this work we restricted our attention to inputs with continuous marginals, which cover a large class of engineering problems. Extensions of R-vines to discrete (*e.g.*, categorical and count) data have been recently proposed (Panagiotelis et al., 2012, 2017).

The methodology was first demonstrated on a simple horizontal truss model, for which Monte Carlo solutions were computationally affordable, and then replicated on a more complex truss model of a dome. Both structures deflected in response to loads on different nodes. Changing the copula among the loads from the independence to a Gaussian to a tail-dependent C-vine copula significantly changed the statistics of the deflection, in particular its variance and upper quantiles. Taken the vine copula as the true dependence structure among the loads, the independence and Gaussian assumptions thus led to a large mis-estimation of these statistics. The failure probability of the two systems, in particular, was mis-estimated by one to two orders of magnitude. This was true regardless of the particular UQ method used for the estimation. Using instead a vine copula model of the input dependencies and fitting the model to relatively few input observations yielded far better estimates.

These results demonstrate that using a proper dependence model for the inputs can be more critical to high-accuracy estimates of the output's statistics than employing a superior UQ algorithm. Our framework encompasses both aspects, allowing highly flexible probabilistic models of the input to be combined with virtually any UQ technique available to

date.

Selecting a vine that properly represents the dependencies of multivariate inputs may be challenging. We discussed and employed existing methods to perform inference on available data. When the dimension of the input is large or the parametric families of pair copulas considered for the vine construction are many, fully automated inference may become computationally prohibitive. A-priori information on the input's statistics may be used to ease the selection, for instance by Bayesian methods (Gruber and Czado, 2015). The problem of selecting suitable vines, however, remains open in very high dimension (say, > 50) or on very large samples. Also, computing the Rosenblatt and inverse Rosenblatt transforms in these cases may be computationally demanding or lead to numerical instability. Additional work is foreseen to address these challenges.

Acknowledgements

The work has been funded by the ETH Foundation through the ETH Risk Center Seed Project SP-RC 07-15 "Copulas for Big Data Analysis in Engineering Sciences", and by the RiskLab from the Department of Mathematics of the ETH Zurich. The authors thank Moustapha Maliki for providing access to the Abaqus implementation of the dome model and to the UQLink module of UQLAB needed to run it, and for helpful discussions on the interpretation of the dome response. Conflicts of interest: none.

References

References

- O. Ditlevsen, H. Madsen, Structural reliability methods, J. Wiley and Sons, Chichester, 1996.
- M. Lemaire, Structural reliability, Wiley, 2009.
- R. Lebrun, A. Dutfoy, Do Rosenblatt and Nataf isoprobabilistic transformations really differ?, Prob. Eng. Mech. 24 (2009) 577–584.
- A.-M. Hasofer, N.-C. Lind, Exact and invariant second moment code format, J. Eng. Mech. 100 (1974) 111–121.
- B. Fiessler, H.-J. Neumann, R. Rackwitz, Quadratic limit states in structural reliability, Journal of Engineering Mechanics 105 (1979) 661–676.
- R. Melchers, Structural reliability analysis and prediction, John Wiley & Sons, 1999.

- I. Papaioannou, W. Betz, K. Zwirgmaier, D. Straub, MCMC algorithms for subset simulation, *Probabilistic Engineering Mechanics* 41 (2015) 89–103.
- R. Li, R. Ghanem, Adaptive polynomial chaos expansions applied to statistics of extremes in nonlinear random vibration, *Prob. Eng. Mech.* 13 (1998) 125–136.
- M. Rosenblatt, Remarks on a multivariate transformation, *Ann. Math. Stat.* 23 (1952) 470–472.
- A. Nataf, Détermination des distributions dont les marges sont données, *C. R. Acad. Sci. Paris* 225 (1962) 42–43.
- R. Nelsen, *An introduction to copulas*, Springer Series in Statistics, Springer-Verlag New York, 2006. doi:10.1007/0-387-28678-0.
- H. Joe (Ed.), *Dependence modeling with copulas*, CRC Press, 2015.
- K. Goda, Statistical modeling of joint probability distribution using copula: Application to peak and permanent displacement seismic demands, *Structural Safety* 32 (2010) 112–123.
- K. Goda, S. Tesfamariam, Multi-variate seismic demand modelling using copulas: Application to non-ductile reinforced concrete frame in Victoria, Canada, *Structural Safety* 56 (2015) 39–51.
- I. Zentner, A general framework for the estimation of analytical fragility functions based on multivariate probability distributions, *Structural Safety* 64 (2017) 54–61.
- C. Michele, G. Salvadori, G. Passoni, R. Vezzoli, A multivariate model of sea storms using copulas, *Coastal Engineering* 54 (2007) 734–751.
- M. Masina, A. Lamberti, R. Archetti, A copula based approach for estimating the joint probability of water levels and waves, *Coastal Engineering* 97 (2015) 37–52.
- R. Montes-Iturrizaga, E. Heredia-Zavoni, Reliability analysis of mooring lines using copulas to model statistical dependence of environmental variables, *Applied Ocean Research* 59 (2016) 564–576.
- H. Joe, Families of m -variate distributions with given margins and $m(m-1)/2$ bivariate dependence parameters, in: L. Rüschendorf, B. Schweizer, M. D. Taylor (Eds.), *Distributions with fixed marginals and related topics*, volume 28 of *Lecture Notes–Monograph Series*, Institute of Mathematical Statistics, 1996, pp. 120–141.
- T. Bedford, R. M. Cooke, Vines – a new graphical model for dependent random variables, *The Annals of Statistics* 30 (2002) 1031–1068.

- K. Aas, Pair-copula constructions for financial applications: A review, *Econometrics* 4 (2016) 43.
- F. Wang, H. Li, Towards reliability evaluation involving correlated multivariates under incomplete probability information: A reconstructed joint probability distribution for isoprobabilistic transformation, *Structural Safety* 69 (2017a) 1–10.
- F. Wang, H. Li, Stochastic response surface method for reliability problems involving correlated multivariates with non-gaussian dependence structure: Analysis under incomplete probability information, *Computers and Geotechnics* 89 (2017b) 22–32.
- K. Aas, C. Czado, A. Frigessi, H. Bakken, Pair-copula constructions of multiple dependence, *Insurance: Mathematics and Economics* 44 (2009) 182–198.
- U. Schepsmeier, Efficient information based goodness-of-fit tests for vine copula models with fixed margins, *Journal of Multivariate Analysis* 138 (2015) 34–52.
- A. Sklar, Fonctions de répartition à n dimensions et leurs marges, *Publications de l'Institut de Statistique de L'Université de Paris* 8 (1959) 229–231.
- P. Embrechts, A. McNeil, D. Straumann, Correlation and dependence in risk management: Properties and pitfalls, in: *Risk Management: Value at Risk and beyond*, Cambridge University Press, 1999, pp. 176–223.
- M. Scarsini, On measures of concordance, *Stochastica* 8 (1984) 201–218.
- M. D. Taylor, Multivariate measures of concordance, *Annals of the Institute of Statistical Mathematics* 59 (2007) 789–806.
- C. Klüpperberg, C. Czado, Vine copula models, <https://www.statistics.ma.tum.de/forschung/vine-copula-models/>, no date. [Online; accessed 21-September-2017].
- D. Kurowicka, R. M. Cooke, Distribution-free continuous bayesian belief nets, in: A. Wilson, N. Limnios, S. Keller-McNulty, Y. Armijo (Eds.), *Modern Statistical and Mathematical Methods in Reliability*, World Scientific Publishing, 2005, pp. 309–322.
- A. Min, C. Czado, Bayesian model selection for d-vine pair copula constructions, *Canadian Journal of Statistics* 39 (2011) 239–258.
- L. Gruber, C. Czado, Sequential bayesian model selection of regular vine copulas, *Bayesian Analysis* 10 (2015) 937–963.
- I. H. Haff, K. Aas, A. Frigessi, On the simplified pair-copula construction – simply useful or too simplistic?, *Journal of Multivariate Analysis* 101 (2010) 1296–1310.

- J. Stöber, H. Joe, C. Czado, Simplified pair copula constructions — limitations and extensions, *Journal of Multivariate Analysis* 119 (2013) 101–118.
- S. Grønneberg, N. Hjort, The copula information criteria, *Scand. J. Stat.* 41 (2014) 436–459.
- J.-D. Fermanian, An overview of the goodness-of-fit test problem for copulas, in: P. Jaworski, F. Durante, W. K. Härdle (Eds.), *Copulae in Mathematical and Quantitative Finance*, volume 213, Springer, 2012, pp. 61–89.
- H. Manner, Estimation and Model Selection of Copulas with an Application to Exchange Rates, Research Memorandum 056, Maastricht University, Maastricht Research School of Economics of Technology and Organization (METEOR), 2007.
- O. Morales-Nápoles, Counting vines, in: D. Kurowicka, H. Joe (Eds.), *Dependence Modeling: Vine Copula Handbook*, World Scientific Publisher Co., 2011, pp. 189–218.
- D. L. Applegate, R. E. Bixby, V. Chvátal, W. J. Cook, *The Traveling Salesman Problem: A Computational Study*, New Jersey: Princeton University Press, 2006.
- J. Kirk, Traveling salesman problem – genetic algorithm, <https://ch.mathworks.com/matlabcentral/fileexchange/13680-traveling-salesman-problem-genetic-algorithm>, 2014.
- J. Dißmann, E. C. Brechmann, C. Czado, D. Kurowicka, Selecting and estimating regular vine copulae and application to financial returns, *Computational Statistics and Data Analysis* 59 (2013) 52–69.
- M. D. McKay, R. J. Beckman, W. J. Conover, A comparison of three methods for selecting values of input variables in the analysis of output from a computer code, *Technometrics* 2 (1979) 239–245.
- V. Romanovsky, On the moments of the standard deviation and of the correlation coefficient in samples from normal, *Metron* 5 (1925) 3–46.
- R. Ghanem, P. Spanos, *Stochastic Finite Elements : A Spectral Approach*, Courier Dover Publications, 2003.
- D. Xiu, G. Karniadakis, The Wiener-Askey polynomial chaos for stochastic differential equations, *SIAM J. Sci. Comput.* 24 (2002) 619–644.
- S. Marelli, B. Sudret, UQLab user manual – Polynomial chaos expansions, Technical Report, Chair of Risk, Safety & Uncertainty Quantification, ETH Zurich, 2017. Report # UQLab-V1.0-104.
- O. Le Maître, O. Knio, H. Najm, R. Ghanem, A stochastic projection method for fluid flow – I. Basic formulation, *J. Comput. Phys.* 173 (2001) 481–511.

- A. Keese, H. Matthies, Numerical methods and Smolyak quadrature for nonlinear stochastic partial differential equations, Technical Report, Technical Report, Technische Universität Braunschweig, 2003.
- D. Xiu, Numerical methods for stochastic computations – A spectral method approach, Princeton University press, 2010.
- M. Berveiller, B. Sudret, M. Lemaire, Stochastic finite elements: a non intrusive approach by regression, *Eur. J. Comput. Mech.* 15 (2006) 81–92.
- A. Doostan, H. Owhadi, A non-adapted sparse approximation of PDEs with stochastic inputs, *J. Comput. Phys.* 230 (2011) 3015–3034.
- J. Jakeman, M. Eldred, K. Sargsyan, Enhancing ℓ_1 -minimization estimates of polynomial chaos expansions using basis selection, *J. Comput. Phys.* 289 (2015) 18–34.
- G. Blatman, B. Sudret, Adaptive sparse polynomial chaos expansion based on Least Angle Regression, *J. Comput. Phys* 230 (2011) 2345–2367.
- M. Hohenbichler, R. Rackwitz, First-order concepts in system reliability, *Structural Safety* 1 (1983) 177–188.
- A. Der Kiureghian, P. Liu, Structural reliability under incomplete probability information, *J. Eng. Mech.* 112 (1986) 85–104.
- Matlab version 9.0.0.341360 (R2016a), The Mathworks Inc., Natick, Massachusetts, 2016.
- M. Kurz, Vine copulas with matlab, <https://ch.mathworks.com/matlabcentral/fileexchange/46412-vine-copulas-with-matlab>, 2015.
- S. Marelli, B. Sudret, UQLab: A framework for uncertainty quantification in Matlab, in: *Vulnerability, Uncertainty, and Risk (Proc. 2nd Int. Conf. on Vulnerability, Risk Analysis and Management (ICVRAM2014), Liverpool, United Kingdom)*, 2014, pp. 2554–2563.
- M. Smith, ABAQUS/Standard User’s Manual, Version 6.9, Simulia, 2009.
- A. Kaveh, S. Talatahari, Particle swarm optimizer, and colony strategy and harmony search scheme hybridized for optimization of truss structures, *Computers and Structures* 87 (2009) 267–283.
- A. Panagiotelis, C. Czado, H. Joe, Pair copula constructions for multivariate discrete data, *J. Amer. Statist. Assoc.* 107 (2012) 1063–1072.
- A. Panagiotelis, C. Czado, H. Joe, J. Stöber, Model selection for discrete regular vine copulas, *Computational Statistics & Data Analysis* 106 (2017) 138–152.